FAST PYROLYSIS OF OLEAGINOUS YEAST

FOR BIOFUEL PRODUCTION

Pongsatorn Poopisut

A Thesis Submitted in Partial Fulfillment of the Requirement for the

Degree of Master of Science in Biotechnology

Suranaree University of Technology

Academic Year 2019

การแยกสลายยีสต์น้ำมันด้วยความร้อนแบบเร็วสำหรับ

การผลิตเชื้อเพลิงชีวภาพ

นายพงศธร ภูพิศุทธิ์

FAST PYROLYSIS OF OLEAGINOUS YEAST FOR

BIOFUEL PRODUCTION

Suranaree University of Technology has approved this thesis submitted in partial fulfillment of the requirements for a Master's Degree.

Thesis Examining Committee

_____

(Assoc. Prof. Dr. Mariena Ketudat-Cairns)

Chairperson

_____

(Assoc. Prof. Dr. Apichat Boontawan)

Member (Thesis Advisor)

_____

(Assoc. Prof. Dr. Adisak Pattiya)

Member

_____ _____

(Assoc. Prof. Flt. Lt. Dr. Kontorn Chamniprasart) (Prof. Dr. Neung Teaumroong)

Vice Rector for Academic Affairs Dean of Institute of Agricultural Technology

and Internationalization

พงศธร ภูพิศุทธิ์ : การแยกสลายยีสต์น้ำมันด้วยความร้อนแบบเร็วสำหรับการผลิตเชื้อเพลิง
ชีวภาพ (FAST PYROLYSIS OF OLEAGINOUS YEAST FOR BIOFUEL
PRODUCTION) อาจารย์ที่ปรึกษา : รองศาสตราจารย์ ดร.อภิชาติ บุญทาวัน, 94 หน้า

        ถังหมักชีวภาพขนาด 500 ลิตรถูกใช้ในศึกษาการผลิตพลังงานเชื้อเพลิงชีวภาพรุ่นที่ 3 โดย
ยีสต์น้ำมัน *Rhodosporidium paludigena* ยีสต์สายพันธุ์นี้มีไตรกลีเซอไรด์สูงและกรดไขมันหลัก
ประกอบด้วย กรดไขมันที่มีคาร์บอนอะตอม 16 และ 18 ซึ่งมีลักษณะคล้ายกับกรดไขมันที่ถูกพบใน
พืช ยีสต์น้ำมัน *R. paludigena* ถูกหมัก โดยใช้มันสำปะหลังเป็นสารตั้งต้น เซลล์ยีสต์ถูกแยกออก
โดยกระบวนการกรอง จากนั้นล้างและถูกทำให้แห้งโดยใช้เทคโนโลยีทำแห้งแบบพ่นฝอย
กระบวนการแยกสลายตัวด้วยความร้อนแบบเร็วของยีสต์น้ำมันถูกศึกษาที่อุณหภูมิ 400-600 องศา
เซลเซียส เพื่อหาอุณภูมิที่เหมาะสมสำหรับการผลิตน้ำมันชีวภาพและถ่านชีวภาพ ผลการทดลอง
แสดงให้เห็นว่าในสภาวะที่เหมาะสมของการสลายตัวของยีสต์น้ำมันได้รับน้ำมันเชื้อเพลิงชีวภาพ
สูงสุดที่ 60 % ภายใต้อุณหภูมิ 550 องศาเซลเซียส การจำลองการกลั่นน้ำมันเชื้อเพลิงชีวภาพจาก
สภาพที่เหมาะสมโดยเทคนิคแก๊สโครมาโตกราฟฟีพบว่าน้ำมันนี้ประกอบด้วย แนฟทาหนัก 2.6 %,
เคโรซีน 20.7 %, ไบโอดีเซล 24.3 % และน้ำมันเตา 52.4 % นอกจากนี้น้ำมันเชื้อเพลิงชีวภาพที่
อุณหภูมิที่ 550 องศาเซลเซียส ได้ถูกนำไปกลั่นที่อุณภูมิ 150 องศาเซลเซียสโดยเครื่องกลั่น
ระยะทางสั้น ผลิตภัณฑ์ที่ได้จากการกลั่นวัดได้ 49 % ผลิตภัณฑ์เชื้อเพลิงเหลวนี้สามารถใช้สำหรับ
พาหนะและอุตสาหกรรมต่างๆ เช่น การสันดาปของเครื่องยนต์ หม้อต้มไอน้ำ กังหันไอน้ำ และอื่นๆ

สาขาวิชาเทคโนโลยีชีวภาพ   ลายมือชื่อนักศึกษา _____
ปีการศึกษา 2562   ลายมือชื่ออาจารย์ที่ปรึกษา _____
                                                              ลายมือชื่ออาจารย์ที่ปรึกษาร่วม_____

PONGSATORN POOPISUT : FAST PYROLYSIS OF OLEAGINOUS

YEAST FOR BIOFUEL PRODUCTION. THESIS ADVISOR : ASSOC.

PROF. APICHAT BOONTAWAN, Ph.D., 94 PP.

FAST PYROLYSIS/OLEAGINOUS YEAST/BIO JET PRODUCTION/

FERMENTATION

A third-generation biofuel production was investigated in a 500-L bioreactor
using an oleaginous yeast *Rhodosporidium paludigena*. This strain contains high
triglyceride content, and the main fatty acids are C16 and C18 which are very similar
to fatty acids found in vegetable oils. The *R. paludigena* yeast was cultured using
cassava starch as substrate. The cells were separated using microfiltration then
washed and spray dried. Bio-oil and biochar were obtained from fast pyrolysis of the
dried yeast powder. The fast pyrolysis process was operated at 400-600 °C to obtain
the optimal temperature for bio-oil and biochar production. The result of this research
showed that the optimal condition of fast pyrolysis giving the highest bio-oil yield of
60% was 550 °C. Simulated distillation gas chromatography technique was used to
classified the biofuels content from 550 °C fast pyrolysis. The results showed that the
contents were 2.6 % heavy naphtha, 20.7 % kerosene, 24.3 % biodiesel and 52.4 %
fuel oil. Moreover, the bio-oil obtained was further distilled at 150 °C using short path
distillation technique. The distillate product from short path distillation was measured

to be 49 % wt. This liquid fuel product could be used for transport and industries such as combustion engines, boilers, turbines, etc.

School of Biotechnology

Academic Year 2019

Student's Signature _____

Advisor's Signature_____

Co-advisor's Signature _____

ACKNOWLEDGEMENT

I would like to express my deep and sincere gratitude to my research advisor, Assoc. Prof. Dr. Apichat Boontawan for giving me the opportunity to do research and providing invaluable guidance throughout this research. He has taught me the methodology to carry out the research and to present the research works as clearly as possible. It was a great privilege and honor to work and study under his guidance.

Besides my advisor, I would like to thank my thesis co-advisor, Assoc. Prof. Dr. Mariena Ketudat-Cairns for the continuous support of my Master' Degree study and research.

I thank the Bio-energy and Renewable resources Research Unit, for their support to do this work. I thanks Assoc. Prof. Dr. Adisak Pattiya for their genuine support in Bio-energy and Renewable resources Research Unit to complete this thesis successfully.

I would like to say thanks to my friends and research colleagues, for their constant encouragement.

Finally, my thanks go to all the people who have supported me to complete the research work directly or indirectly.

<div align="right">Pongsatorn Poopisut</div>

CONTENTS

CONTENTS (Continued)

LIST OF TABLES

LIST OF FIGURES

Figure **Page**

LIST OF FIGURES(Continued)

LIST OF FIGURES(Continued)

LIST OF FIGURES(Continued)

LIST OF ABBREVIATIONS

ETS	=	Emission Trading Scheme
FAMEs	=	Fatty Acid Methyl (or ethyl) Esters
ASTM	=	American Society of Testing and Materials
VCR	=	Volume Concentration Ratio
SDGC	=	Simulated Distillation Gas Chromatography
MF	=	Microfiltration
RO	=	Reverse Osmosis
ESP	=	Electrostatic Precipitator
SEM	=	Scanning Electron Microscope
XRD	=	X-Ray Diffractometer
FTIR	=	Fourier-Transform Infrared Spectroscopy
BET	=	Brunauer, Emmett and Teller
HHV	=	High Heating Value
SPD	=	Short Path Distillation

CHAPTER I

INTRODUCTION

1.1 Significance of study

The energy consumption trends rising and most energy has been generated from fossil fuel, while a few bio fuel has been used as shown in Figure 1.1 (a). The fossil fuel is depleted according to heavily use by industry, transportation, and etc. (Figure 1.1 b). Thus, renewable fuels play an important role to substitute fossil fuels. One of the green energy is biofuel, the biofuel had been produced from biomass as raw material.

Commercial aviation is an industry that releases a lot of emission of pollution by using fossil fuel, and it will increase in the near future. The energy consumption affects global warming because energy consumption has been increasing, but fossil fuel has limited and is running out soon. Thus bio fuel has been researched and developed to substitute fossil fuel. Besides that, European Union (EU) make some rule about transportation of each airline of aviation called "Emission Trading Scheme or ETS". The EU use ETS to control the greenhouse effect. Thus, the airlines are interested to use bio jet fuel combined with fossil fuel (http://www.ptgenergy.co.th). NASA confirm bio jet fuel can reduce jet emission, the mixture of bio jet fuel with fossil fuel can reduce emission around 50-70% (https://www.flyingmag.com/nasa-confirms-biofuels-reduce-jet-emissions).

Vegetable oils have been used for biodiesel production because these oils have high triacylglycerides (TAG) content. Biodiesel is produced from trans esterification of TAG by using an alcohol, either ethanol or methanol. Moreover biodiesel was produced by using oils accumulating of microorganism such as microalgae, bacterial, yeast and other fungi (Irnayuli, 2014). The advantages of microorganism for biodiesel producing are high production rate, low agricultural area, easy harvesting.
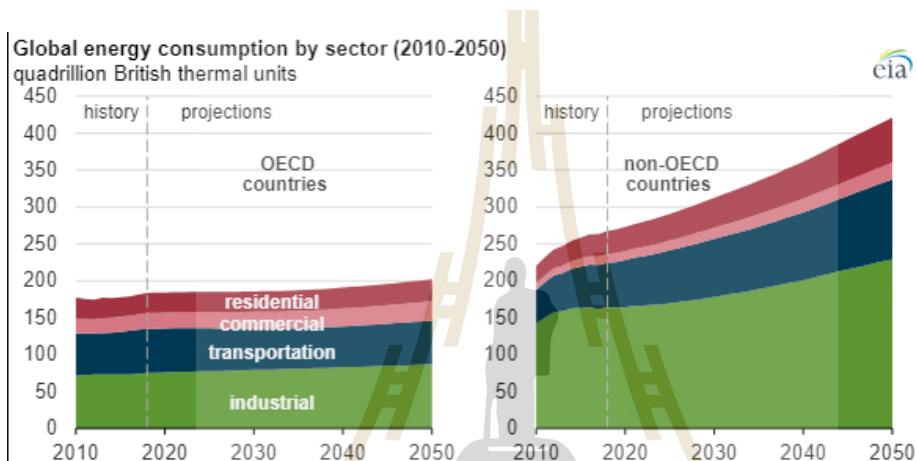
(a)
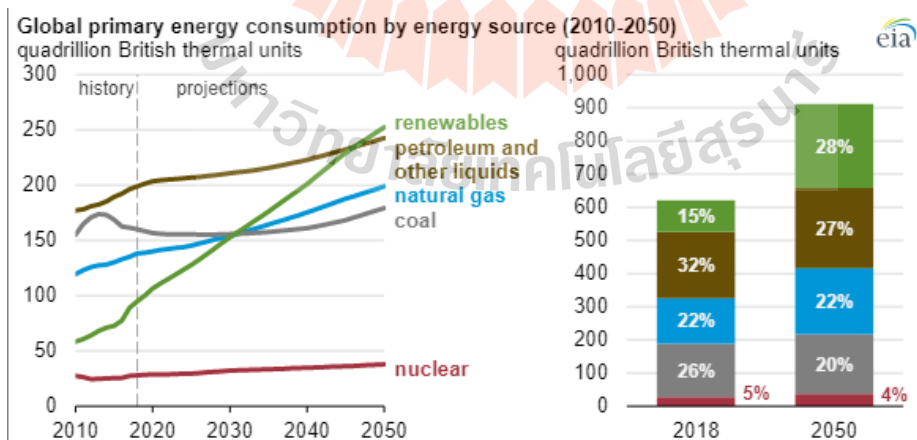
(b)

Figure 1.1 (a) Trend of world energy consumption, (b) type of world energy consumption. (U.S. Energy Information Administration, *International Energy Outlook 2019* Reference case**.**

1.2 Research objective

1.2.1 To study optimal condition of *Rhodosporidium paludigena* fermentation.

1.2.2 To compare membrane separation between dead end and crossflow filtration

1.2.3 To study optimal temperature for high conversion of spray drying of oleaginous yeast *R. paludigena* broth.

1.2.4 To study optimum condition and parameter for high conversion of fast pyrolysis process by using oleaginous yeast *R. paludigena* as raw material.

1.2.5 To compare properties and characteristic of product from biofuel production with standard fuel.

1.3 Research hypothesis

Oleaginous yeast contains high lipid in cell, the long chain fatty acid can be cracked by fast pyrolysis process. The high bio-oil yield is obtained at optimal condition of fast pyrolysis. The high yield of bio jet fuel and biodiesel can be distillated by short path distillation.

1.4 Scope and limitation of study

Oleaginous yeast fermentation was investigated in a 500-L bioreactor. Both dead end and cross flow filtration were used for cell harvesting. Spray drying was used for cell drying with different temperatures.

The dried yeast powder was used as raw material in fast pyrolysis process with different temperatures. The physical and chemical properties of bio-oils were analyzed and compared with standard fuel. The bio-oil at optimal temperature was simulated distillation curve by gas chromatography technique.

1.5 Expected results

1.5.1 High lipid accumulation and yield of fermentation of oleaginous yeast *R. paludigena*.

1.5.2 High performance of membrane separation could be obtained from cross flow filtration.

1.5.3 High yeast powder yield in spray drying unit.

1.5.4 High bio-oil yield could be obtained from fast pyrolysis process.

1.5.5 The properties of bio-oil could be similar with petroleum.

1.5.6 The high yield of distillated product could be obtained from short path distillation.

1.5.7 The physical and chemical properties of distillated product could be similar with standard fuel.

CHAPTER II

LITERATURE REVIEW

2.1 Biofuel production

2.1.1 Biofuel generation

Biofuel is fuel that produce from biomass through process, Biofuel is classified to 3 generations as follow:

1. First generation biofuel

The first generation biofuels are biofuels that produce from food crops grown on farm land. Biofuel production has increased in the past. Some agricultural commodities like maize (corn), sugar cane, or vegetable oil can be used either as food, feed, or to make biofuels. However, food versus biofuel is the problem about the risk of diverting food crops for biofuel production and that damage to food supply. Moreover, this problem affects the biofuel and food price. The relative strengths of these positive and negative impacts vary in the short and long terms.

2. Second generation biofuel

The second generation biofuels are fuels manufactured from agricultural residues or various types of non-food biomass according to the concern about first generation biofuels. The second generation biofuels are made from different feedstock, and require different technologies to produce them. The second generation feed stocks

include lignocellulosic biomass or woody crops, agricultural residues, and waste. The second generation technology have been developed, which enable non-food feedstock to make the biofuels.

The conceptual second-generation biofuel production is to extend the amount of biofuel that can be produced sustainably by using biomass consisting of the residual non-food parts of current crops, such as stems, leaves and husks that are left behind the food crop production. Moreover, other crops that are not used for food purposes (non-food crops), such as grass, jatropha, whole crop maize, straw and also industry waste such as woodchips, skins and pulp from fruit pressing, etc (https://en.wikipedia.org/wiki/Second-generation_biofuels)

The problem of second generation biofuel processes are extraction of useful feedstock from woody or fibrous biomass. All plants contain lignin, hemicellulose, and cellulose, respectively. These are complex carbohydrates (molecules based on sugar). The useful sugars are locked in by lignin, hemicellulose and cellulose. Lignocellulosic feedstock is made by freeing the sugar molecules from cellulose using enzymes, steam heating, or other pre-treatments. These sugars can then be fermented to produce ethanol in the same way as first-generation bioethanol production. The by-product of this process is lignin. Lignin can be burned as a carbon neutral fuel to produce heat and power for the processing plant. Thermochemical processes (liquefaction) in hydrothermal media can produce oily liquid products from a wide range of feedstock that has a potential to replace or augment fuels. However, these liquid products fall short of diesel or biodiesel standards. Upgrading liquefaction products through one or many physical or chemical processes may improve properties for use as fuel.

3. Third generation biofuel

The problem of second generation biofuel process is pretreatment of lignocellulosic feedstock. In addition, the production cost is not worth for investment. The third generation biofuels are alternative fuels produced from microorganism. One of bioresources is microalgae which are naturally found in the marine environment. There are more than 300,000 species of microalgae. The several species of microalgae can produce oil in their body. Some species of microalgae have a short time during their growth (Firoz Alam et al., 2015). Moreover, some species of yeast collect high lipid in the cell called "oleaginous yeast". The lipid content in some stains of oleaginous yeast can be up to 70 % (Shields-Menard et al., 2018). The culture of microorganism can help to retrench cultivated area. The current biofuel yields from various biomasses are shown in Table 2.1 It shows huge potential of micro-organism compared to other biomasses.

Table 2.1 the comparison of oil yield of different biomass (Firoz Alam et al., 2015).

Oil yield	Litre/Hectare/Year
Soybean	400
Sunflower	800
Calona	1600
Jatropha	2000
Palm oil	6000
Microorganism	60,000-240,000

2.1.2 Type of liquid biofuel production

1. Biodiesel production

Biodiesel is an alternative fuel that has characteristic resemble with petroleum diesel. Biodiesel has been produced through the chemical reaction of transesterification of triglyceride, and alcohol such as methanol and ethanol. Thus, the biodiesel consist mostly of fatty acid methyl esters (FAMEs) or ethyl esters (FAEEs). Feedstocks for the biodiesel production include animal fat, vegetable oil such as soy, rapeseed, jatropha, mahua, mustard, flax, sun flower, hemp, and palm oil. Moreover, microorganisms can also be used for example algae and oleaginous yeast. The main process steps require to synthesis biodiesel are as follow:

1.1 Feedstock pretreatment

Normal feedstocks used in biodiesel synthesis are recycle vegetable oil, vegetable oil, and tallow. The recycle oil are removed impurities such as dirt and water by refinement process. Water need to be removed because the saponification (hydrolysis) reaction of triglycerides instead of transesterification, soap is formed to replace of biodiesel.

1.2 Chemical reaction

The biodiesel is produced from reaction of triglyceride (fat and oil) with short chain alcohol (typically methanol or ethanol), and the by-product is glycerol. Under normal condition, this reaction occur very slowly. The catalyst and heating are used for help to speed up the reaction. Common based-catalysts for transesterification include sodium hydroxide, potassium hydroxide, and sodium methoxide.Almost of all biodiesel is produced from vegetable oil by using based-catalysts technique in commercial scale.

The based-catalysts transesterification is described as follow:

R_1, R_2, R_3 = Hydrocarbon chain ranging from 15 to 21 carbon atoms
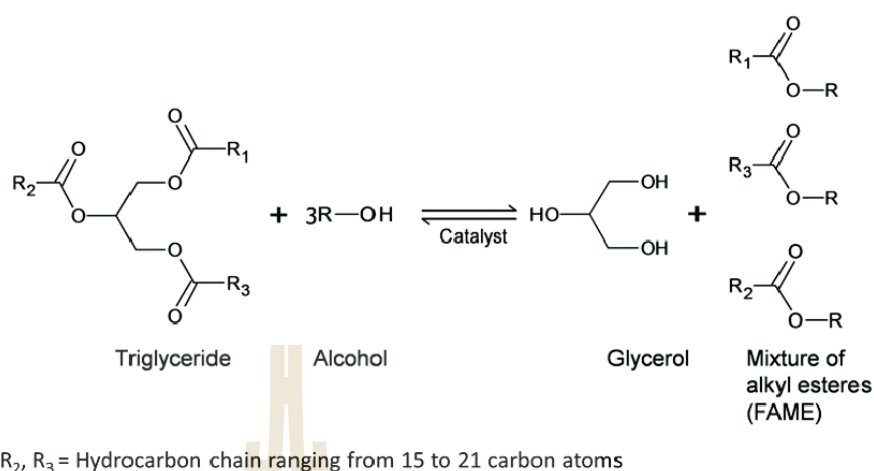
Figure 2.1 Transesterification of biodiesel.

1.3 Purification

The byproduct in this process such as soap, glycerol, exceed alcohol, and some amount of water. All of these byproducts need to be removed prior to use. For example crude biodiesel was purified by dry washing technology and membrane separation as shown in figure 2.2, dry washing process was achieve via application of adsorbents such as activated carbon, amberlite, pulolite, cellulosics, magnesol, trisyl, activated fiber, and activated clay. Which adsorbed glycerol, methanol and etc. Membrane technology was used for removal impurities (Atadashi, 2015).
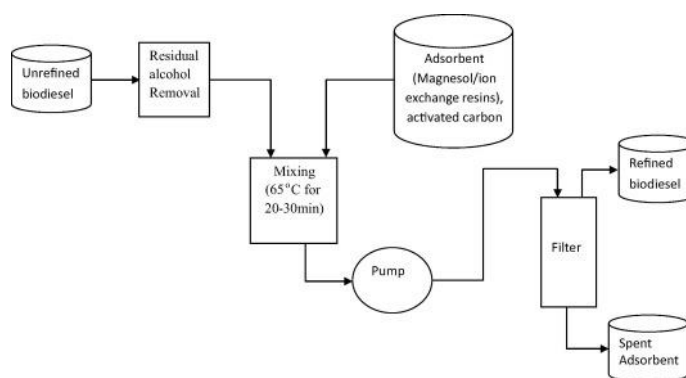
Figure 2.2 Schematic diagram of dry washing technology and membrane separation (Atadashi, 2015)

2. Fischer Tropsch

Fischer-Tropsch process is a chemical reaction that convert small molecule or gas mixture called syngas such as carbon monoxide, hydrogen with catalyst to liquid hydrocarbon. The gas mixture is obtained by biomass gasification. The syngas was fed into Fischer-Tropsch step. The reaction occurs in metal catalyst at high temperature. The characteristic of product depends on the ratio of syngas (H_2/CO) and catalyst. The Fischer-Tropsch process is shown in Figure 2.3 and it has three main steps as followed:

Firstly, syngas production or gasification, syngas or hydrogen and carbon monoxide are prepared, and purified from resources such as coal, natural gas and biomass. The fuel from biomass is called biomass to liquid (BTL).

Secondly, Fischer-Tropsch liquid synthesis, the product from this step is called FT wax or syn-crude, the characteristic of hydrocarbon depends on the ratio of syngas, catalyst and conditions.

Finally, refining and upgrading product, the syn-crude is separated, and then it is upgraded by structure conversion such as treating, cracking, and isomerization.
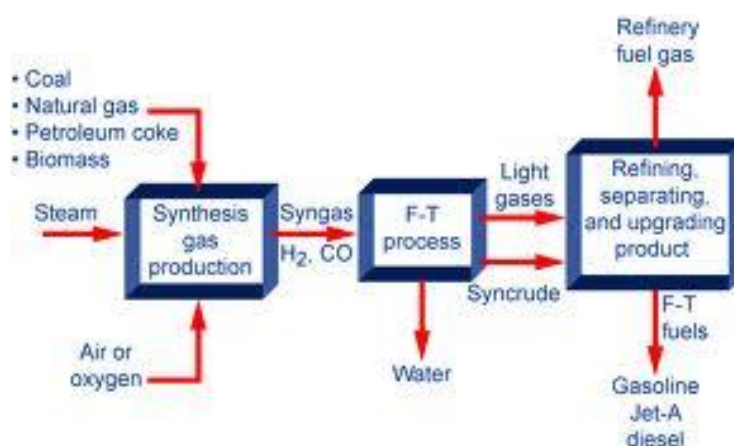
Figure 2.3 Fischer-Tropsch process

The more useful reactions produce alkanes as follows:

$$(2n + 1)\, H_2 + n\, CO \rightarrow C_nH_{2n+2} + n\, H_2O$$
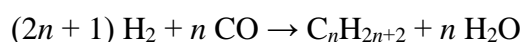
After syn-crude is upgraded and distillated. The products are obtained from Fischer-Tropsch process. It is pure fuel without sulfur and nitrogen. However, the Fischer-Tropsch process have to use high energy, that occur a lot of by-products, and the yield of jet fuel is low.

3. Hydro-processed Renewable biofuel

Nowadays, bio-oils has been produced and developed to substitute crude oil or petroleum. Bio-oils is produced from biomass or organic materials such as triglyceride, cellulosic biomass, lignocellulosic biomass, sugar, ethanol, and etc. Therefore, chemical structure of bio-oils is similar to the fossil fuel. Thus, the conceptual bio-oils production is like oil refinery process, the four main steps are

1. Conversion, actually the biomass or organic materials have different chemical structures. Thus, each process depends on the type of materials. Nevertheless, the main idea of conversion is cracking or breaking down long chain hydrocarbon to short chain hydrocarbon. The thermal cracking has been used in bio-oil production by using triglyceride, cellulosic, and lignocellulosic biomass as material.

2. Treating is catalytic chemical reaction, and it is used to remove oxygen in chemical structure of bio-oils. Because chemical structure of fossil fuel is low oxygen content, thus the properties of bio-oils is similar to the fossil fuel.

3. Reforming is catalytic chemical reaction used to covert chemical structure of bio oil.

4. Modification or upgrading, low temperature alkylation is a key reaction step used to

produce C_8-C_{15} aromatic before cyclic alkane conversion in bio-oil from straw stalk (Wong *et al.* 2015).

The triglyceride feedstock includes cooking oil, jatropha oil, algae oil, animal fat. That can be converted into biofuels by hydroprocessing. The hydro-processed renewable biofuel consists of the chemical conversion of triglyceride and fatty acid through hydrodeoxygenation. The hydro-processed renewable biofuel is shown in Figure 2.4. The oxygen content was removed by additional hydrogen. The triglyceride and fatty acid are converted to linear long chain hydrocarbon with hydrogen and solid catalyst at high temperature and pressure. The deoxygenation and decarbonation reaction are occurred generating water, carbon dioxide, and carbon monoxide as by products.
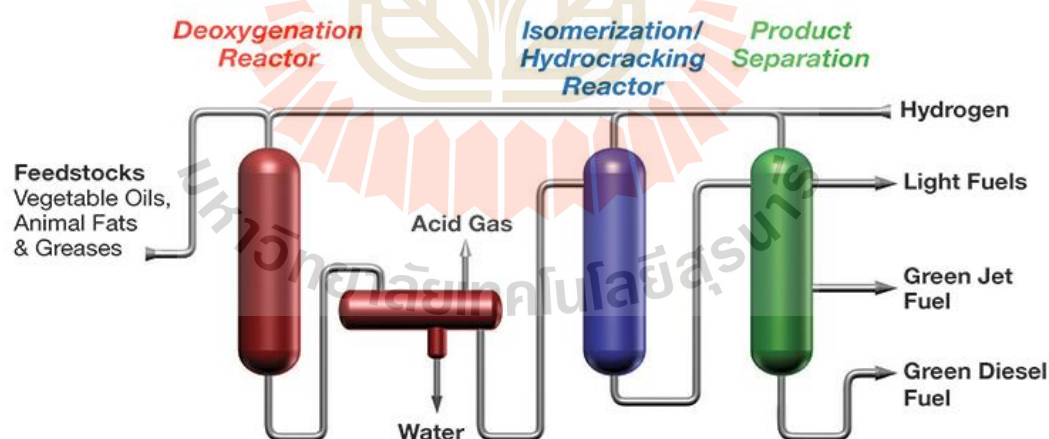
Figure 2.4 Hydro-processed *Renewable* biofuel.

The linear long chain hydrocarbons are generated in the first reactor, and enter to isomerization/ hydrocracking reactor. The isomerizing and cracking are

occurred. The chain hydrocarbons are range of C8 to C18. Light fuel, naphtha, green diesel are produced, and then the fuels are separated by distillation.

2.2 Oleaginous yeast

Yeast is a single celled microorganism that is classified as member in the fungus kingdom. Yeasts have been availed for biotechnological application for thousands of years; for example, the yeast *Saccharomyces cerevisiae* had been used for producing beer, bread, wine, and other product (Irnayuli, 2014). In addition, some species of yeast can accumulate high lipid in the cell called "oleaginous yeast". Genetic engineering has been used to develop high lipid accumulation in oleaginous yeast. The oleaginous yeast *Yarrowia lipolytica* was improved by the metabolic engineering of the lipid synthesis pathway. Simultaneous overexpression of Stearoyl-CoA desaturase (SCD), Acetyl-CoA carboxylase (ACC1), and Diacylglyceride acyl-transferase (DGA1) in *Y. lipolytica* yielded an engineered strain exhibiting highly desirable phenotypes of fast cell growth and lipid overproduction including high carbon to lipid conversion yield (84.7% of theoretical maximal yield), high lipid titers (≈55g/L), and enhanced tolerance to glucose and cellulose-derived sugars. Moreover, the engineered strain shows a three folds growth advantage over the wild type strain. A maximal lipid productivity of 1 g/L/h is obtained during the stationary phase (Qiao, 2015). The oil is accumulated in microbes called Single cell oil (SCO). Oleaginous yeast can convert substrate such as carbon dioxide, sugar, and organic acid to SCO. Both oleaginous and non-oleaginous yeasts contain lipid such as diacylglycerols or diglyceride (DAG), triacyl-glycerols or triglyceride (TAG), free fatty acid, sterol, carotenoids. sphingolipid, and phospholipids, respectively (Irnayuli, 2014). The main fatty acid in oleaginous yeast *Yarrowia*

lipolytica are oleic acid (C18:1), linoleic acid (C18:2n6), and palmitic acid(C16:0) (Breil C. et al.,2016). Oleaginous yeast accumulates intracellular triglyceride in lipid body as much as 80-90% of total lipid. The average oil yield from various yeast species range between 37-65 % according Table 2.2

Table 2.2 Lipid content in various oleaginous yeast (Shields-Menard et al., 2018).

Yeast	Lipid content (%w/w)
Lipomyces starkeyi	52.6
Cryptococcus curvatus	34.6
Yarrowia lipolytica	58.5
Rhodotorula glutinis	53.0
Cryptococcus. echinula	37.6
Cryptococcus albidus	65.0
Cryptococcus potothecoides	46.1
Rhodosporidium toruloides	37.6
Lipomyces starkeyi	38.0

The most common fatty acids are 16-18 carbon in length (C16 and C18), and in the form of either saturated (no double bonds, such as C16:0) or monounsaturated (one double bonds, such as C18:1). The most common fatty acid (FA) of oleaginous yeasts are C18:1 (oleic acid), C16:0 (palmitic acid), and C18:0 (stearic acid), respectively. Table 2.3 shows fatty acid composition of various oleaginous yeasts.

In the development of bioprocess, many oleaginous yeasts are non-pathogenic or non toxic,, and are generally recognized as safe (GRAS). They are shear strength to mixing, high growth rate, easy to harvest by the mean of filtration, and easy to extract

the oil from cell. So, it is suitable to develop the biofuels production in commercial scale.

Table 2.3 Fatty acid comparison of *R. paludigena* with different stains of yeast.

fatty acid composition %	*Cryptococcus curvatus*	*Yarrowia lipolytica*	*Rhodotorula kratochvilovae*	*Rhodosporidium paludigena*
C16:0	16.74	9.15	18.63	21.32
C16:1	2.69	5.92	0.50	0.82
C18:0	7.25	3.37	5.68	10.80
C18:1	22.66	50.71	53.82	47.94
C18:2	30.69	30.02	20.34	3.06
C18:3	0.45	0.81	0.55	0.36
C20:0	0.80	-	-	0.32
Other	18.72	0.02	0.48	15.38
References	Chang *et al*., (2011)	Breil *et al*., (2016)	Jiru *et al*., (2016)	This work

The biotic component of oleaginous yeast is lipid. The lipid are hydrophobic molecules or biomolecule that is soluble in non polar solvent such as chloroform, ether, benzene, and hexane. In lipid molecule, some part is polar molecule that connect with non polar molecules. So, it is amphiphile or amphiphithic molecule. Lipid have important functions as the structure of cell membrane, energy storage, etc. Lipid can be classified into 3 groups.

1. Simple lipid is ester of fatty acid and long chain alcohol such as fats, wax, and oil.

2. Compound lipid is ester of fatty acid, chain alcohol, and other compounds such Derived lipid is organic compound of hydrolysis of simple lipid and compound lipid

such as fatty acid, glycerol, mono glycerol, triglyceride, steroids, cholesterol, carotenoid, and etc.

3. Fatty acid is carboxylic acid (-COOH) with long aliphatic chain (-R). The part of carboxylic group is polar molecule, and the aliphatic chain is non polar molecule. The most carbon atom of fatty acid is even number (C12-C24). Fatty acid contains single bond or double bond thus fatty acid have 2 types.

3.1 Saturated fatty acid (SFA) is fatty acid that have single bond. Saturated fatty acid is found in plant and animal but it is found in animal more than plant such as lard. The saturated fatty acid can be synthesized in body. The most common saturated fatty acid is palmitic acid that is found in palm oil, and stearic acid. The general formula is $C_nH_{2n}O_2$.

3.2 Unsaturated fatty acid (UFA) is fatty acid that have double bond in some part. As a result, unsaturated fatty acid reacts faster than saturated fatty acid. Some unsaturated fatty acid can not be synthesized in body. So, it is called essential fatty acid. The most unsaturated fatty acid is oleic acid and linoleic acid. The general formula is $C_nH_{2n-2}O_2$. In addition, unsaturated fatty acid have 2 types

3.2.1 Mono unsaturated fatty acid (MUFA) have a double bond in a molecule such as palmitoleic (16:1n-7), and oleic(18:1n-9).
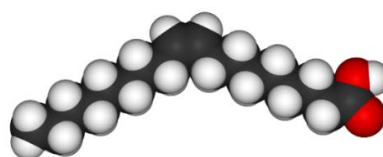
Oleic (18:1(n-9))

3.2.2 Polyunsaturated fatty acid (PUFA) have double bonds in a molecule
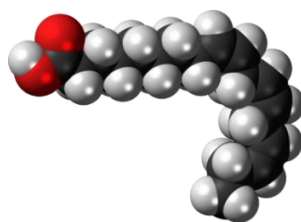
α-Linolenic acid(18:3 (*n*−6))

2.3 Fermentation of oleaginous yeast

Oleaginous yeast is one of microbial oil or called single cell oils (SCO), that can produce high lipid and accumulate in the cell. The oleaginous yeast was isolated from the soil in litchi orchard, longan orchard, carambola orchard, and wood (Pan Li-Xia et al., 2008). The oleaginous yeast have many strains, some strain had been improved by genetic engineering. Both oleaginous yeasts (*Yarrowia lipolytica, Rhodotorula glutinis, Trichosporon cutaneum, Candida sp.*) and non oleaginous yeast were studied about lipid accumulation, and increase lipid accumulation by increasing C/P ratio with higher C/N ratio. The C/N ratio of 30 was found to lead to higher biomass content and the total lipid content increased significantly with higher C/P ratio. With higher ratios of both C/N and C/P, the content of monounsaturated fatty acids (FAs) in cell lipids increased while polyunsaturated FAs decreased. Oleaginous yeast species had a lower proportion of unsaturated FAs (approx. 80 %) than non-oleaginous strains (approx. 90 %). At a C/N ratio of 30 and C/P ratio 1043, *T. cutaneum* produced a high amount of ω-6 unsaturated linoleic acid, the precursor of some prostaglandins, leukotrienes, and thromboxanes, while *Candida sp.* And *K. polysporus* accumulated a

high content of palmitoleic acid (Kolouchová I. et al., 2016). Moreover the growth characteristics and composition during the life cycle of isolated strain of *Debaryomyces etchellsii* were studied under nitrogen limiting conditions. This oleaginous yeast was grown in batch flask or bioreactor cultures. The *D. etchellsii* were cultured on a nitrogen limiting medium (NLM) containing (in g/L): Glucose 50; $(NH_4)_2SO_4$ 0.5; Yeast extract 1; KH_2PO_4 12; Na_2HPO_4 12; Mg $SO_4.7H_2O$ 1.5; $CaCl_2.2H_2O$ 0.1; $MnSO_4.5H_2O$ 0.0001; $CuSO_4.5H_2O$ 0.0001; $Co(NO_3)_3.3H_2O$ 0.0001; $ZnSO_4.7H_2O$ 0.001. The initial pH of the medium was 6 ± 0.1 after autoclaving. Flasks experiments were performed in duplicate, in 250 cm^3 Erlenmeyer flasks, containing 50 cm^3 of the above NLM. After sterilization (at 115 °C for 20 min). The bioreactor batch of total volume 3.7 L was used to ferment in working volume 1.8 L. the bioreactor was sterilized at 121 °C for 2 h and kept at room temperature for 48 h to ensure sterility of the medium. The culture vessel was inoculated with 200 cm^3 of inoculum. The cultivation conditions were as follows: dissolved oxygen was maintained above 20% of saturation. The pH of the medium was 6 and automatically controlled by adding 1 M NaOH or 0.5 M H_2SO_4. The fermentation temperature was automatically controlled at 28 °C and the agitation rate was 3 Hz. Antifoam was added when needed (Fatma Arous *et al*., 2015).

The growth of oleaginous yeast depends on species, and environmental condition such as temperature, pH, substrate, C/N ratio and oxygen. this parameter influence to efficiency of lipid accumulation. The optimal condition was repoted in *Rhodosporidium toruloides* by NLM composed of 70 g/L glucose, 0.75 g/L yeast extract, 0.55 g/L $(NH_4)_2SO_4$, 0.4 g/L KH_2PO_4, 2 g/L $MgSO_4•7H_2O$, with a pH of 5.5 using shaking flask cultivation at 150 rpm and 28 °C. This oleaginous yeast can produce a lipid quantity of 9.26 g/L, which was 71.30 % of the dry biomass (13.33 g/L) after 168 h of cultivation

(Kraisintu P *et al*., 2010). The optimal condition and NLM of *R. toruloides* is referenced to use for fermentation of *R. paludigena* in this experiment.

The growth of oleaginous yeast or other microorganisms in batch culture can be modeled with four different phases as follow in Figure 2.5
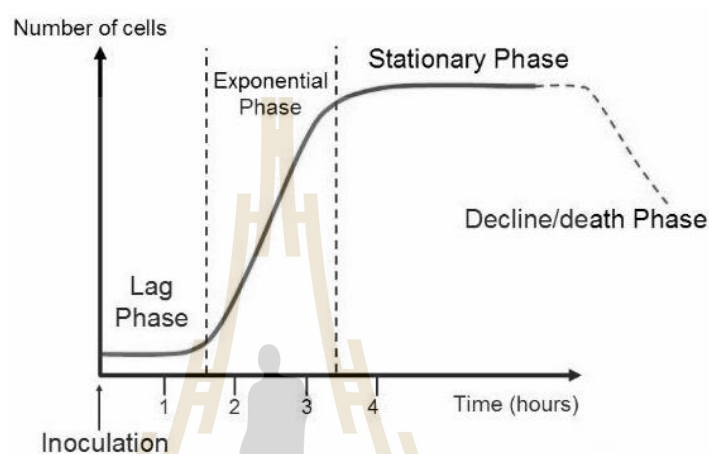
Figure 2.5 Yeast or other microorganism growth curve

1. Lag phase

When yeast is inoculated into new medium, cells change very little because the cells do not immediately reproduce in a new medium. the cells are metabolically active and increase only in cell size. They synthesize the enzymes and factors needed for cell division and population growth under their new environmental conditions. During this period, called the lag phase.

2. Log phase (exponential phase)

After lag phase, yeast cells enter the log phase or exponential phase. This phase is a period characterized by cell doubling. Exponential growth cannot continue indefinitely, because the medium is soon depleted of nutrients and enriched with wastes.

3. Stationary phase

The stationary phase is often due to a growth-limiting factor such as the depletion of an essential nutrient, and the formation of an inhibitory product such as an organic acid. Stationary phase results from a situation in which growth rate and death rate are equal.

4. Death phase (decline phase)

During this phase, cells die, this could be caused by lack of nutrients, inhibitory product, environmental temperature above or below the tolerance band for the species, or other injurious conditions.

Growth rate modeling

Growth rate of yeast or microorganism depend on concentration of cells. It can describe as follow:

$$\frac{dx}{dt} = \mu x$$

Integration of equation

$$\int_{x_0}^{x_t} \frac{dx}{x} = \int_0^t \mu dt$$

$$\ln(x_t) - \ln(x_0) = \mu(t - 0)$$

$$\ln\left(\frac{x}{x_0}\right) = \mu t$$

x = concentration of cells at time

x_0 = initial concentration

μ = specific growth rate

t = time

For exponential phase the specific growth rate is maximum as follow:

$$\ln\left(\frac{x}{x_0}\right) = \mu_{max}t$$

Doubling time (t_d) is solve by assume that cells increase double. Thus, $x = 2x_0$

$$\ln\left(\frac{2x_0}{x_0}\right) = \mu_{max}t_d$$

$$\ln(2) = \mu_{max}t_d$$

$$t_d = \frac{\ln(2)}{\mu_{max}}$$

$$t_d = \frac{0.693}{\mu_{max}}$$

**This equation can be used perfectly for log phase.

2.4 Cell harvesting

After fermentation, oleaginous yeast cell must to be separated from broth before it is washed by water during harvesting process. Water in the cell is removed by drying after it is concentrated by membrane technology. The separation is used in harvesting such as centrifugation and membrane separation.

2.4.1 Centrifugation

Centrifugal force is applied to use in cell harvesting. The centrifuge is a device that separate particles from solid-liquid mixture though a use of rotor. Although product from centrifugation is more concentrated than membrane technology but the centrifugation can not separate only cell, thus product have impurity more than concentrate from membrane technology.

2.4.2 Membrane technology

Membrane separation is type of filtration that separate from mixture by through thin porous sheet or membrane. the fluid can through membrane called "Permeate or Filtrate" and parts can not pass called "Retentate or Concentrate". Some particle accumulate on surface of membrane called "cake". The membrane filtration process is shown in Figure 2.6
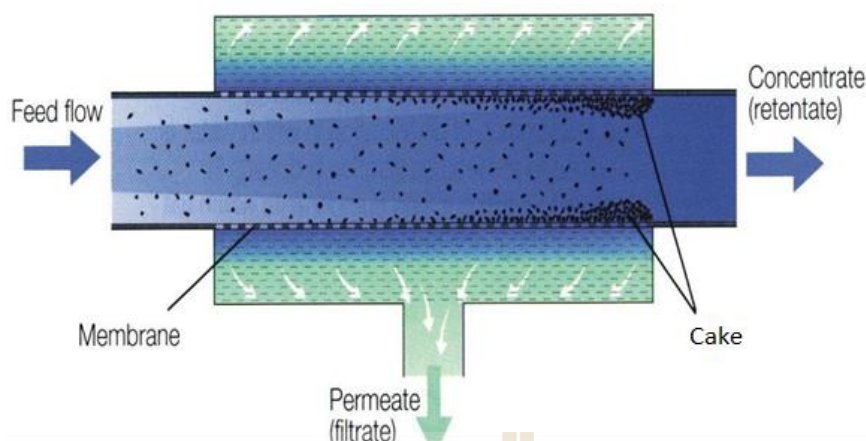
Figure 2.6 Membrane filtration.

Membrane separation processes differ based on separation mechanisms and size of the separated particles. The type of membrane filtration is divided by pore size of membrane. The widely used membrane filtration include micro filtration, ultrafiltration, nanofiltration, reverse osmosis and etc. The Figure 2.7 shows the comparison of membrane techniques.
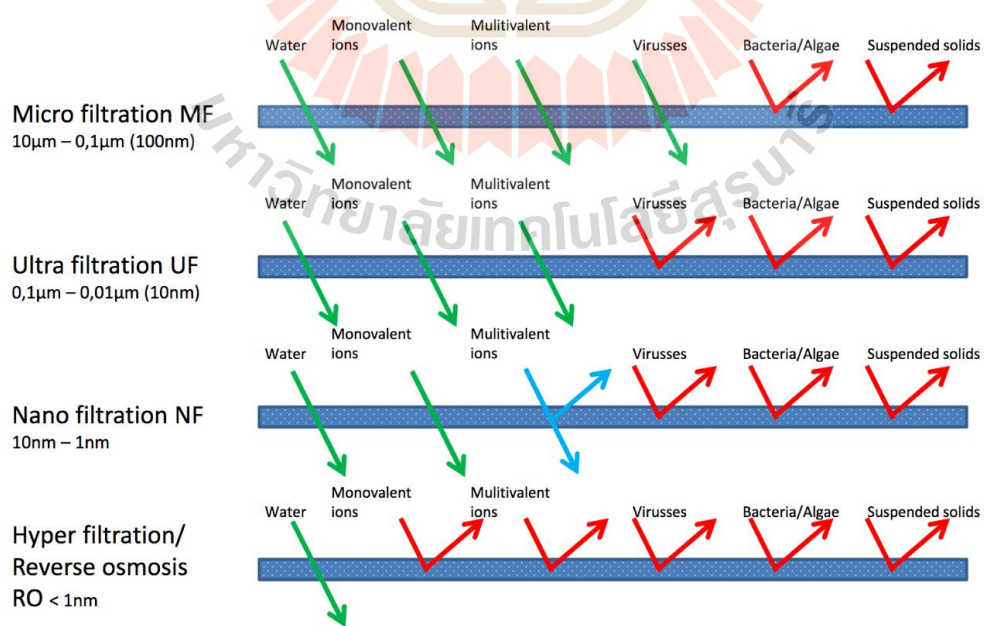
© Logisticon Water Treatment b.v.

Figure 2.7 Comparison of membrane techniques.

Normally, there are two main flow configurations of membrane processes, That include and dead end and cross flow filtration as follow:

1.Dead end filtration

Dead end filtration is one of membrane separation technique that feed stream is perpendicular with surface area of membrane as shown in Figure 2.8
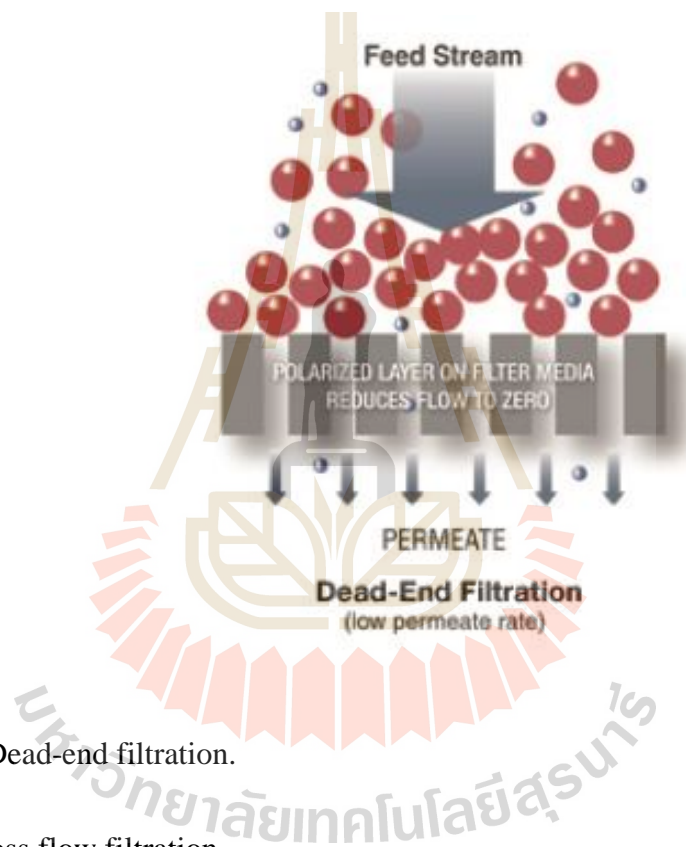
Figure 2.8 Dead-end filtration.

2. Cross flow filtration

Cross flow filtration is type of membrane filtration that direction of feed flow is tangential with surface area of membrane as shown in Figure 2.9
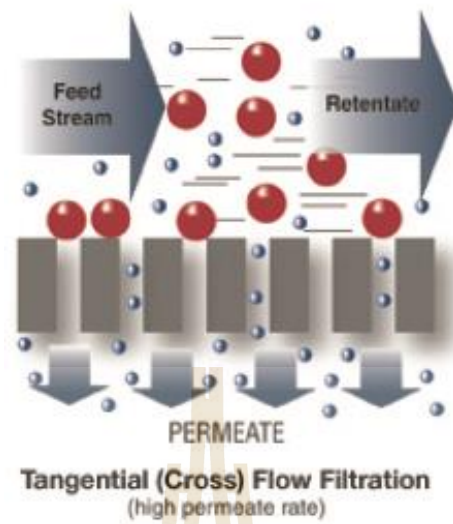
Figure 2.9 Cross flow filtration.

In this experiment, theory of membrane is applied with Darcy's law as follow :

$$Q = \frac{k\Delta p}{\mu l} \qquad (1)$$

When Q = Volumatic filtration flowrate (m^3/s)

k = Darcy's law permeability (m^2)

Δp = Pressure drop across the filter medium (Pa)

μ = Viscosity of the broth (kg/m.s)

l = Thickness of the filter medium (m)

The permeability and thickness of filter can be combined into a medium resistance term.

$$R_m = \frac{l}{k}$$

When R_m = medium resistance (m^{-1})

Equation (1) can be written as;

$$Q = \frac{A\Delta p}{\mu R_m} \quad \text{or} \quad Q = \frac{dV}{dt} = \frac{A\Delta p}{\mu R_m}$$

At any instant during filtration basing on the Darcy's law, rate of filtration is given by the equation;

$$J = \frac{1}{A}\frac{dV}{dt} = \frac{\Delta p}{\mu R} \qquad (2)$$

When J = Flux, and $R = R_m + R_c$

In this case R is a combination of resistance of filter medium (R_m) and resistance of cake solids (R_c). And the resistance of cake solids (R_c) can be written as;

$$R_c = \alpha p_c \frac{V}{A} \qquad (3)$$

When ρ_c is the mass of dry cake solids per volume of filtrate and α is specific cake resistance. Combination of equation (2), and (3) results in the following equation;

$$\frac{1}{A}\frac{dV}{dt} = \frac{\Delta p}{\mu \left[\alpha p_c \frac{V}{A} + R_m\right]} \qquad (4)$$

And integration of the eqution (4) results in;

$$\frac{At}{V} = \frac{\mu\alpha p_c}{2\Delta p}\left(\frac{V}{A}\right) + \frac{\mu R_m}{\Delta p} \tag{5}$$

2.5 Cell drying

Drying is step to adjust and control moisture level in solid particle through heat transfer. The drying unit is one of most common and important in industries. Since it is used in every plant that produce or handle solid material in the form of powder and granules. The effectiveness of drying processes can have a large impact on product quality and process efficiency in the factories. For example, in the pharmaceutical industry, the drying process can impact after manufacturing steps, including powder flow, tableting or encapsulation, stabilize moisture-sensitive materials and that can affect critical quality of the final dosage form. In this work, the drying process was tested using 2 different types of dryer as followed;

1. Freeze dryer

Freeze drying or lyophilization is a water removal process typically used to preserve perishable materials, to extend shelf life or make the material more convenient for transport. Freeze drying works by freezing the material, then reducing the pressure and adding heat to allow the frozen water in the material to sublimate. The freeze drying is more suitable for products sensitive to temperature and operating time is longer than other machine. For example, In the pharmaceutical process, freeze drying is used for lyophilised powders production. The size distribution of powder particles from freeze

drying was affected by the nanocrystal concentration and the drug to stabilizer ratio (Touzet *et al*.,2018). A freeze drying is shown in Figure 2.10
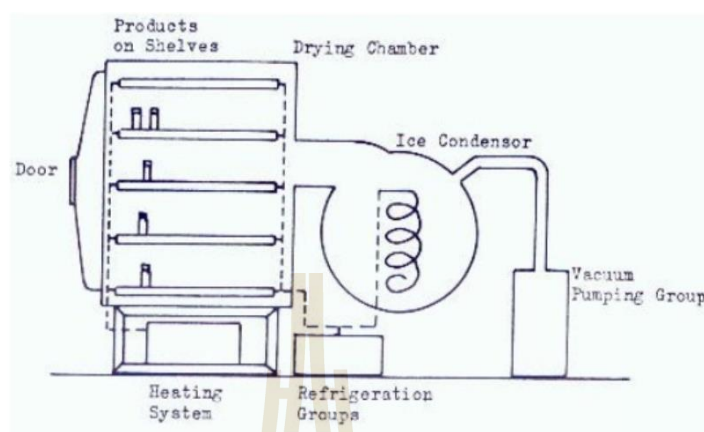
Figure 2.10 An industrial freeze dryer.

2. Spray drying

Continuous dryers are mainly used in chemical and food industries, due to the large volume of product that needs to be processed. Most common are continuous fluid-bed dryers and spray dryers. There are other dryers, depending on the product, that can be used in certain industries.

Spray dryers are the most widely used in chemical, dairy, agrochemical, ceramic and pharmaceutical industries. The spray-drying process can be divided into four sections:1.atomization of the fluid, 2. mixing of the droplets, 3. drying, and, 4. removal and collection of the dry particles. Spray drying unit is shown in Figure 2.11 Atomization is made by feeding liquid mixture through nozzles, or by spinning-disk atomizers. The flow of the drying gas may be concurrent or countercurrent with respect to the movement of droplets, the heat and mass transfer rates are high. The atomization help to increase interfacial surface area, these factors give rise to very high evaporation

rates. The residence time of a droplet in the dryer is only a few seconds (5–30 s). The gas temperatures of 150 to 300 °C is used in process. The complex vegetable extracts, such as coffee or digitalis, milk products, and other labile materials are dried without significant loss of potency or flavor. Freeze concentration combine with spray drying are used to produce feijoa (fruit harvested in South America) powder in temperature of 180-210 °C. The two-fluid nozzle or rotary disk is used for atomization in spray dryer pilot scale(Alejandra Henao *et al*., 2019). The capital and running costs of spray dryers are high, but if the scale is sufficiently large, they may provide the cheapest method.
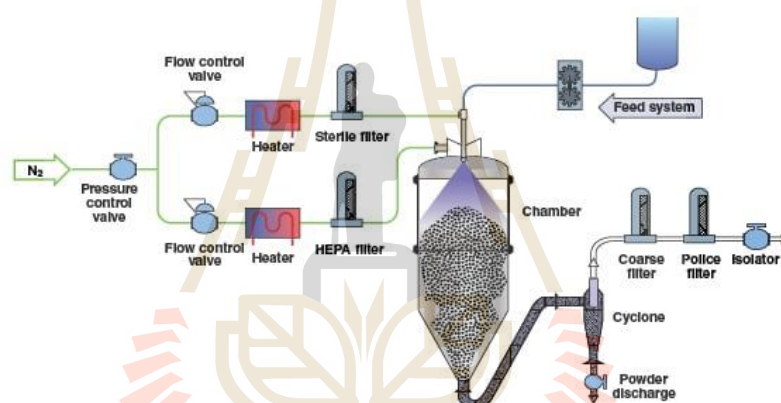
Figure 2.11 Spray drying process

2.6 Fast Pyrolysis of biomass

The biomass can be made into biofuel quickly through a process called fast pyrolysis. The biomass is grinded before being fed into a fast pyrolysis reactor. The biomass is fast heated in the absence of oxygen. The gas product is condensed by a condenser unit. The dark brown liquid is formed called bio-oil or pyrolysis liquid. The by-product is non- condensable gas include carbon dioxide, carbon monoxide, hydrogen. In this case, the bio gas includes ethylene, methane, propane, propylene,

ethane, and others. The solid bio char is separated from bio gas by cyclone unit. The chemical structure of biomass is broken down to small molecules under high temperature depend on types of biomass. The pyrolysis of azolla, sarassum tenerrimum and water hyacinth were heated in the range of 300-450 °C in fixed-bed reactor (Biswas *et al.,* 2017). The continuous fast microwave-assisted pyrolysis reactor was developed to produce bio-oil from rice straw and camellia oleifera shell at 400-600 °C (Wang *et al.,*2018). The biomass from conifers, salix, and reed canary grass was milled and pyrolyzed at 675- 775 °C (Lestander *et al.*,2018). Bio-oils are multi-component mixtures that consisted different size molecules derived primarily from depolymerization and fragmentation reactions of cellulose, hemicellulose, and lignin (Bridgwater, 2004).
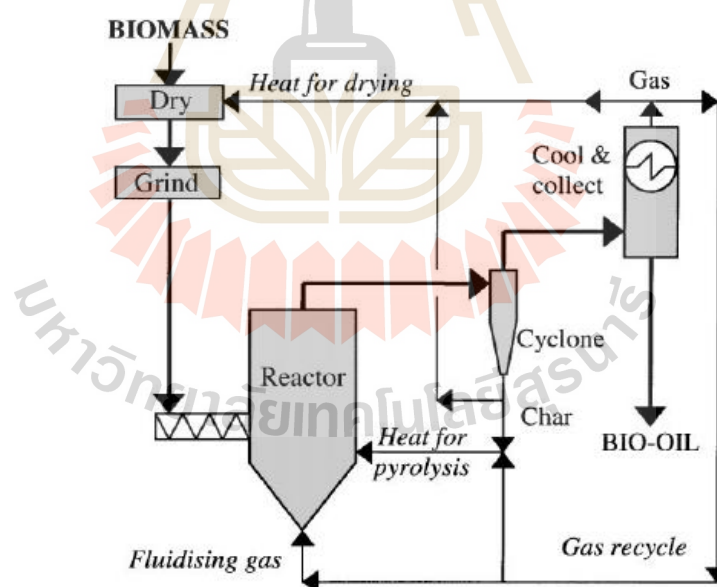
Figure 2.12 Schematic diagram of fast pyrolysis process.

The conceptual fast pyrolysis follows Figure 2.12 In the first step, the biomass need to have low moistures. The biomass is dried before feed to grinder. The biomass is heated by using heat loss from bio gas and bio char. After that, the crushed biomass

is fed to the reactor by screw feeder. The second step, the oxygen in reactor is removed by feeding nitrogen. The reactor is heated combine with heat from bio gas and bio char at temperature around 500 °C. The biomass is started to feed to the reactor. The chemical structure of biomass is converted into bio oil, bio gas and bio char. The products from the fast pyrolysis reactor is fed though a cyclone separator. The bio char is then separated. The heat from cyclone can be used to dry biomass. And then, the bio oil is condensed by using condenser unit. The bio gas can be used as fuel for heating the reactor.

2.7 Simulated distillation gas chromatography (SDGC)

Distillation is one of purifications, that is method to separate the component or substance from liquid mixture by using selective boiling point and condensation. After dried oleaginous yeast trough fast pyrolysis process into bio-oil. Which need to be purified before using it. The bio-oil is analyzed characteristic and components of complex liquid mixture. The distillation curve is one of bio-oil analysis that is a graphical depiction of the boiling temperature of a fluid mixture plotted versus the volume fraction distilled. This volume fraction is usually expressed as a cumulative percent of the total volume. For crude petroleum, the distillation curve can be divided into stages that contain butanes and lighter, gasoline, naphtha, kerosene, gas-oil, and residue. The temperature at each of these cuts or regions provides an idea of the volatility of each cut. Thus, the relative difference between light crude and heavy crude can be "read" from the distillation curve (Thomas J. Bruno, 2006). Normally, the measurement of distillation curve can be determined by using simple distillation. The apparatus is developed for the measurement of distillation curve as show in Figure 2.13
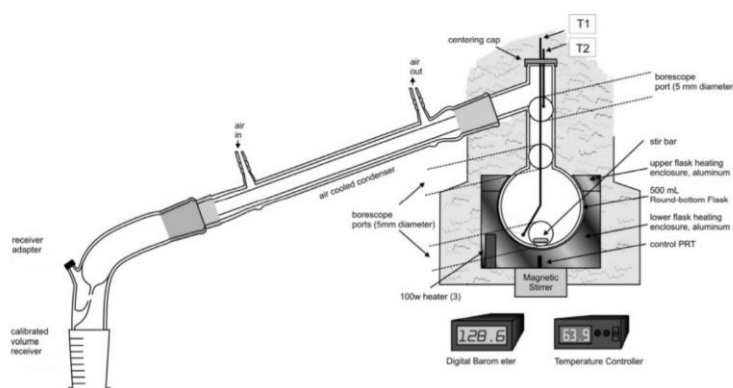
Figure 2.13 The overall apparatus used for the measurement of distillation curves
(Bruno, 2006).

Although distillation curve is measured by the apparatus as Figure 2.13
Moreover, the distillation curve can be determined by Simulated distillation gas
chromatography (SDGC). This technique is a GC method used to characterize
petroleum fractions and products, since it permits the quick determination of their
boiling range distribution. Samples are analyzed on a non polar chromatographic
column that separates the hydrocarbons in order of their boiling points. This analysis
can accurately measure, using a little sample for analysis and quicker than simple
distillation. Thus, SDGC technique is suitable to measure distillation curve of bio-oil
because volume of the sample is limited, and faster than measurement of normal
distillation.

CHAPTER III

MATERIALS AND METHODS

3.1 MATERIALS

3.1.1 Dried oleaginous yeast *R. Paludigena*

The oleaginous yeast *R. paludigena* was isolated by Assoc. Prof. Dr. Mariena Ketudat- Cairns's laboratory. It was fermented in 500-L bioreactor with working volume 350 L. The oleaginous yeast *R. paludigena* cell was separated by membrane separation before spray drying cell. The contents of different fatty acid of oleaginous yeast *R. Paludigena* was specified by Gas Chromatography (Agilent 7890A, USA), that was showed in Figure 3.1.
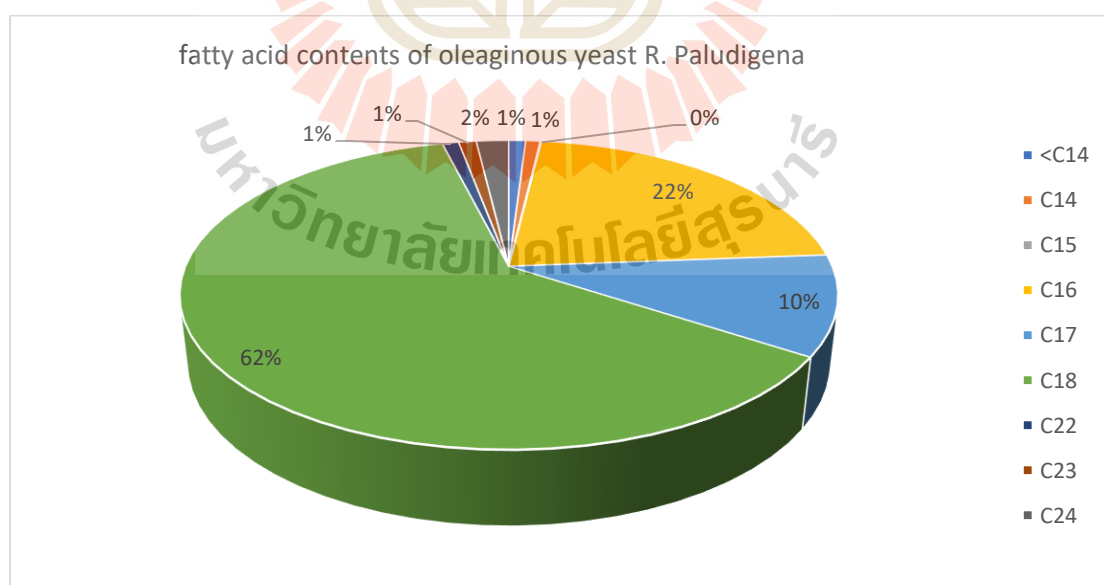
Figure 3.1 Fatty acid contents of dried oleaginous yeast *R. Paludigena* in this experiment.

3.2 EQUIPMENT

All of equipment used in the fermentation, cell harvesting, spray drying, fast pyrolysis and short path distillation process to produce biofuel were shown as follow:

NAMES OF EQUIPMENT	COMPANY
ANALYTICAL BALANCE	PRESICA, USA
PH METER	OHAUS, USA
HOTPLATE AND STIRRER	SCILOGEX, USA
SHAKING INCUBATOR	BENCHMARK SCIENTIFIC, USA
BIOLOGICAL SAFETY CABINET	CRYSTE, KOREA
AUTO CLAVE	CRYSTE, KOREA
FERMENTER 5 L	SATORIUS, GERMANY
FERMENTER 50 L	APICHAT'S LABORATORY
FERMENTER 500 L	BE MARUBISHI, THAILAND
CROSS FLOW MEMBRANE FILTATION	APICHAT'S LABORATORY
MINI SPRAY DRYER B-290	BUCHI, JAPAN
ROTARY EVAPORATOR	BUCHI, JAPAN
DESICCATOR	SANPLATEC, JAPAN
FAST PYROLYSIS REACTOR	ADISAK'S LABOLATORY
SHORT PATH DISTILLATION UNIT	1STLAB, CHINA
GC 7890A	AGILENT, USA
SDGC CP-3800	VARIAN, USA
(CHN) DETERMINATOR SERIES 628	LECO, USA
BOMB COLORIMETER MODEL C 5000 PKG	IKA, GERMANY
SCANNING ELECTRON MICROSCOPE (SEM), MODEL OF JSM 6010LV	JEOL, JAPAN
TGA MACHINE MODEL OF 701	LECO, USA
D2 PHASER XRD	BRUKER, USA
FTIR TENSOR 27-HYPERION	BRUKER, USA
BET INSTRUMENT ASAP 2020 PLUS	MICROMERITICS, USA

3.3 METHODS

3.3.1 Fermentation

The oleaginous yeast $R.$ $paludigena$ was isolated from Assoc. Prof. Dr. Mariena Ketudat- Cairns's laboratory. Figure 3.2 shows the oleaginous yeast $R.$ $Paludigena$ in agar plate, and the optical microscope picture. The seed culture was prepared in a 500 mL medium containing (g/L) of; 70 g glucose, 0.75 g yeast extract, 0. 55 g $(NH_4)_2SO_4$, 0. 4 g KH_2PO_4, and 2. 0 g $MgSO_4.7H_2O$, respectively. Cell cultivation began in a 5-L bioreactor at 30 °C for 48 h. After that, the inoculum was transferred into a 50-L bioreactor at 30 °C for 48 h. The batch experiment was performed in a 500-L bioreactor with 350-L of working volume (BE Marubishi, Thailand). The Figure 3.3 shows the bioreactors used in this work.

Figure 3.2 The oleaginous yeast $R.$ $Paludigena$ and The optical microscope picture.

(a.)   (b.)   (c.)
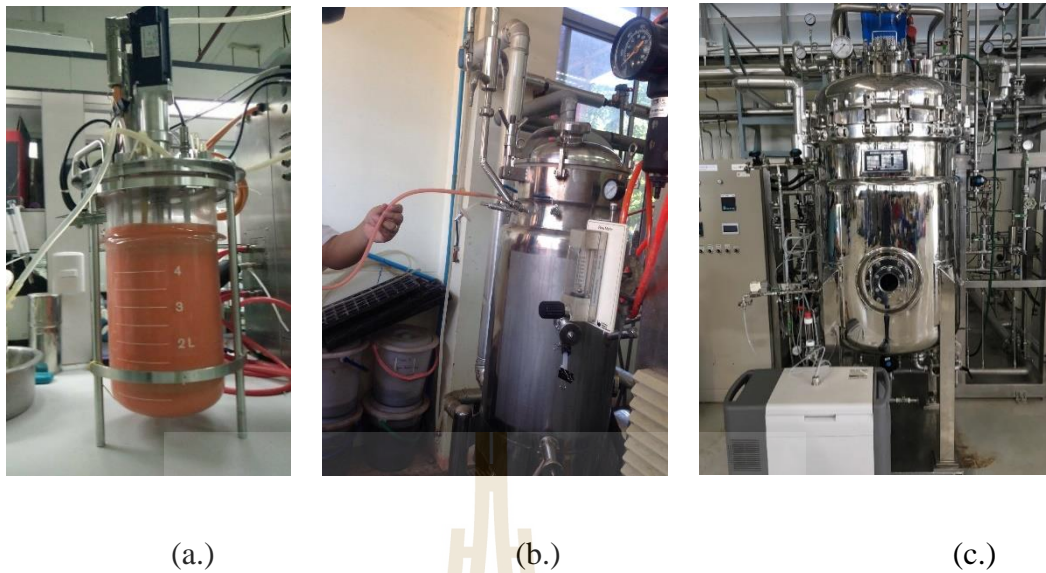
Figure 3.3 Bioreactors in the experiment (a.) 5-L bioreactor (b.) 50-L bioreactor (c.)

500-L bioreactor
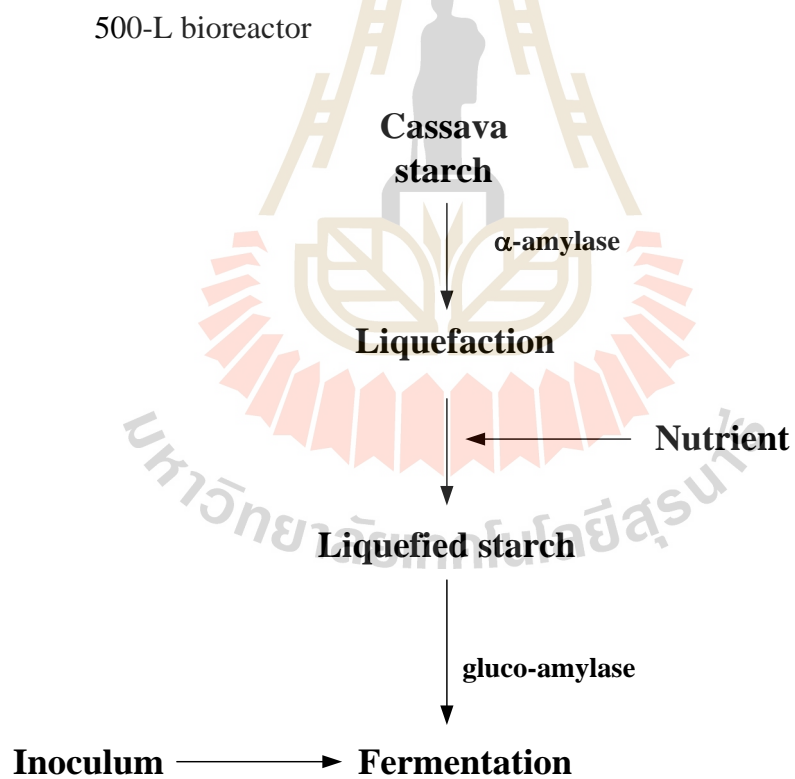
Figure 3.4 The oleaginous yeast *R. Paludigena* fermentation by using cassava starch

as substrate.

The fermentation broth for *R. paludigena* was prepared using mashed cassava starch 80 g/L as the main substrate. The step of fermentation was shown in Figure 3.4 The hydrolyzed starch solution was liquefied by an addition of 0.05 wt% of thermostable α-amylase (Termamyl®, Novozymes, Denmark) volume of 1 ml/L at the working temperature of 90 °C for 2 hrs. Nutrient containing (g/L) of; 0.75 g yeast extract, 0.55 g $(NH_4)_2SO_4$, 0.4 g KH_2PO_4, and 2.0 g $MgSO_4.7H_2O$, respectively. The temperature of the liquefied solution was then decreased to 60 °C before being saccharified by an addition of gluco-amylase (Spirizyme® Fuel, Novozymes, Denmark) at 0.05 wt% volume of 1 ml/L for 12 hrs. After sterilization, the inoculum was transferred aseptically into the bioreactor. During fermentation, temperature was automatically maintained at 30 °C under aerobic condition. The aeration rate was 0.75 VVM with the agitation rate of 150 rpm.

3.3.2 Cell harvesting

After fermentation, oleaginous yeast cell must be separated from broth before being washed by water during harvesting process. Water in the cell was removed by spray drying after it is concentrated by membrane technology. The separation was used in harvesting such as centrifugation and membrane separation.

1. Centrifugation

Centrifugal force was applied to use in cell harvesting. The centrifuge is a device that separate particles from solid-liquid mixture though a use of rotor. The continuous centrifuge has been widely used in chemical and biochemical process for separation in industries. In this work, a disc stack centrifuge was used for separate cell. A stack centrifuge is a special type of preparative centrifuge which is compact in design.

Feed enter from the top of the device and is distributed at the bottom of the disc bowl through a hollow drive shaft. The particles are collected at the periphery of the bowl and discharged from the device in the form of slurry. The liquid flows up the device along the central regions, and is released from the top as shown in Figure 3.5 Disc stack centrifuge are ideally suited for separating particle size 3-30 µm (Amaro *et al.*, 2017).
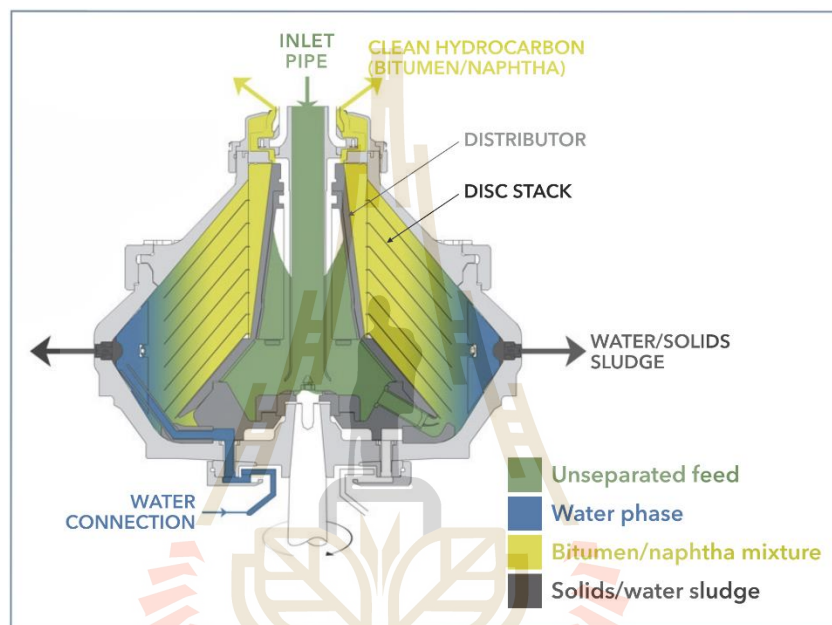
Figure 3.5 The disc stack centrifuge.

2. Membrane separation

Oleaginous yeast cells from fermentation were separated by using not only a cross-flow microfiltration, but also dead-end filtration for study involving the volume concentration ratio (VCR) in the experiment. The cross-flow membrane filtration was shown in Figure 3.6 The cross-flow MF experiment was investigated using a spiral-wound MF element with the nominal pore size of 0.1 µm (Synder's Filtration, USA) installed in a stainless steel housing. The diameter, and the length of the membrane element were measured at 10.2 cm, and 96.5 cm, respectively. The feed spacer was 3

mm, and the total filtration area was 4.27 m^2. A 0.75 kW pump was employed to re-circulate the fermentation broth at the volumetric flow rate of 70 L/min corresponding to the calculated linear flow velocity of 0.09 m/s. The feed temperature was controlled at 30 ^{o}C by using a cooling coil submerged in the MF feed tank. Transmembrane pressure was calculated from the feed, retentate, and permeate pressures using conventional pressure gauges. After each run, the membrane was firstly rinsed with RO water. It was then circulated with 1 wt% NaOH solution for 20 minutes, and rinsed to neutrality with RO water. Finally, it was cleaned with 1.5 wt% phosphoric acid solution before rinsed to pH 7.0 with RO water.

Figure 3.6 The cross-flow MF experiment.

The dead-end filtration experiment was shown in Figure 3.7 The broth (50 mL) was fed in an test cell of dead-end filter. It was investigated using nylon membrane filter pore size of 0.1 µm and 47 mm diameter of membrane (Whatman membrane filter

nylon, Germany). The pressures was applied with pressurized nitrogen gas approximately 1-2 bars. The volume of permeate and time were recorded.
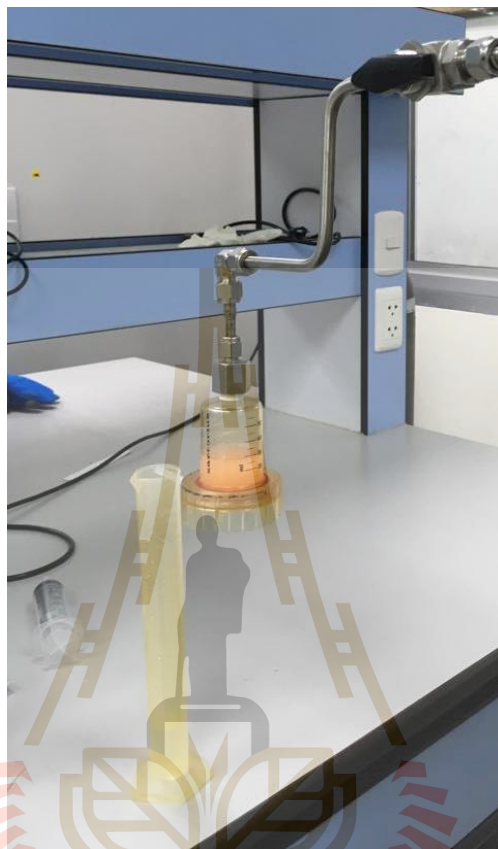
Figure 3.7 The dead-end filtration experiment.

3.3.3 Spray drying

The *R. paludigena* was spray dried at air inlet temperatures of 90 °C, 100 °C , 110 °C, 120 °C and 130 °C respectively. The spray dryer (Buchi's mini spray dryer B-290, Germany) was showed in Figure 3.8 The operating parameters in this work were 470 L/h of air flow rate, 3.5 mL/min feeding rate, and cell concentration of 50 g/L, nozzle size 1.4 mm, aspirator pressure drop -50 mbar. The yeast powders were collected in the auto desiccator with a moisture content within specifications of <10%. Cell

viability was not the concern of this work since the cells were subjected to fast pyrolysis soon after the drying process.

Figure 3.8 A mini spray dryer.

3.3.4 Fast pyrolysis

After spray drying process, a fixed bed fast pyrolysis reactor was set up at Assoc. Prof.Dr. Adisak Pattiya's laboratory, Mahasarakham university. Figure 3.9 shows a fixed bed fast pyrolysis reactor used in this work. The dried oleaginous yeast powder was feed into fast pyrolysis reactor and that reactor was operated at temperatures 400 °C, 450 °C, 500 °C, 550 °C, and 600 °C, respectively. The fiberglass was added in reactor after feeding yeast powder in reactor. Some soot was blocked by fiberglass in the reactor.

Figure 3.9 Fixed bed fast pyrolysis reactor at Mahasarakham university.

The bio-oil was condensed by cooling condenser at -10 °C, and it was trapped by Electrostatic Precipitator (ESP) at 15 kV. The biochar was removed out from fixed bed fast pyrolysis reactor. The non-condensable gas was released into environment.

3.3.5 Short path distillation

Short path distillation is a distillation technique that include the distillate traveling a short distance. The vacuum was extremely low pressure. The bio-oil was heated at 70 °C before it was fed to short path distillation unit. The short path distillation had length between feed and condenser (inside column), distillate product can be condensed in a short distance. It was around a few centimeters. That was called "short path distillation" or "molecular distillation". The molecular (short path) distillation unit model of LAB 1st MD-150 was used for distillated product in this

experiment. The molecular (short path) distillation unit was shown in Figure 3.10 The distillate was obtained from fraction 2 as shown in Figure 3.10(B) and the fraction 3 (Figure 3.10(C)) contained stillage or residue. The bio-oil was tested at 150 °C, vacuum was around 10 mbar, temperature of condenser inside column was around 40 °C. The bio-oil was fed 400 mL. In addition, this instrument had another condenser (outside column), it was set temperature around 10 °C. The condensate was obtained from fraction 1 as shown in Figure 3.10(A). The bio-oil of optimal fast pyrolysis condition was only tested in this experiment because the amount of bio-oil was limited.

Figure 3.10 The molecular (short path) distillation unit model of LAB 1st MD-150.

3.3.6 Analyses

1. Crude fatty acid extraction

The dried oleaginous yeast powder contain moisture lower than 10 %, it was measured crude fatty acid by solvent extraction. In this experiment, the total lipid was extracted by less polar solvent as petroleum ether. The lipid residue was weighed after solvent evaporation.

2. Gas chromatography analysis

A gas chromatography (GC) is an analytical instrument that measure the content of various compounds in the sample and that compound in the sample can be vaporized without decomposition. The oleaginous yeast was analyzed content of fatty acid. Before the fatty acid contents were determined by GC analysis, the fatty acid need to be transformed to fatty acid methyl ester (FAME) by esterification. Firstly, the dried oleaginous yeast powder was extracted by chloroform : methanol (2:1). The extracted yeast oil was prepared 25 mg in test tube for mixing with 0.5 M methanolic NaOH 1.5 mL. then the sample was removed oxygen in the tube by feeding nitrogen gas and it was quickly closed. After that sample was heated around 2 minutes at temperature 80-90 °C and shake it. Then it was left to cool and add BF_3 solution 2 ml. it was removed oxygen again. Then it was heated 30 minutes, and was shaken periodically. When heating finished, it was left to cool. After that it was mixed isooctane 1 mL. and 36 % NaCl solution 5 mL. After phase separation, the upper layer was taken to a new tube. Then repeated extraction, the bottom layer was extracted again by adding isooctane 2 mL, and the upper layer was collected. Finally, the sample was diluted with isooctane 1 mL before it was injected to GC machine.

The sample around 1 µL was injected in GC Agilent 7890A with FID – Detector. The instrument was illustrated in Figure 3.11 The Agilent J&W *CP-Sil 88* column (100m $\times$ 0.25mm $\times$ 0.2um) provides a greater efficiency and resolution for FAME compounds. The injector temperature of 240 °C, split 50:1, detector temperature of 250 °C, and flow rate of 0.4 mL/min. Helium was employed as the carrier gas.

Figure 3.11 GC Agilent 7890A.

3. Gas Chromatography – Mass spectrometry (GC-MS) analysis

Gas Chromatography – Mass spectrometry (GC-MS) is an analytical instrument that combine the features of gas chromatography (GC) and mass spectrometry (MS) to determine compounds in the sample. The result was identified by data base comparison. In this experiment, the bio-oil was diluted with an organic solvent before injection in GC-MS instrument. The Agilent 7000B model was used in this experiment, and was shown in Figure 3.12

Figure 3.12 The Agilent 7000B GC/MS

4. Simulated Distillation Gas Chromatography (SDGC)

Simulated Distillation is a GC method that combine with simulation distillation software used to characterize crude oil sample. This technique was used to measure boiling range distribution. The bio-oils were analyzed at Department of Chemical Technology, Faculty of Science, Chulalongkorn University for boiling range distribution measurement of Simulated Distillation of ASTM D2887. The model of Simulated Distillation Gas Chromatography is Varian CP-3800 that was shown in Figure 3.13

Figure 3.13 The Varian CP-3800.

5. Carbon, Hydrogen, and Nitrogen (CHN) determination

Carbon, Hydrogen, and Nitrogen (CHN) analyzer was used to measure carbon, hydrogen and nitrogen elemental content in samples. The biochar was mashed and sieve size of 1 mm, low moisture and use it around 0.2 g for CHN analysis. Figure 3.14 showed that Carbon, Hydrogen and Nitrogen (CHN) determinator. The instrument utilizes a combustion technique and provides a result within 4.5 minutes for all the elements being determined. The sample was weighed and encapsulated. After that, the sample was placed in the instrument's loader. The sample was transferred to the instrument's purge chamber directly above the furnace, eliminating the atmospheric gases from the transfer process. The sample was then introduced to the primary furnace containing only pure oxygen, resulting in a rapid and complete combustion (oxidation) of the sample. Carbon, hydrogen, and nitrogen present in the sample were oxidized to carbon dioxide (CO_2), water (H_2O), and NO_x .The combustion products are separated by a chromatographic column and detected by the thermal conductivity detector (TCD),

which gives an output signal proportional to the concentration of the individual components of the mixture. The final results were typically displayed in weight percent or parts-per-million.

Figure 3.14 Carbon, Hydrogen and Nitrogen (CHN) determinator series 628 LECO.

6. Automatic calorimeter

The bomb calorimeter is a device that used to measure the energy of combustion. The heat can be determined from temperature change (ΔT). The bio-oil and biochar were determined amount of heat that release from combustion. Figure 3.15 shows the bomb colorimeter IKA model C 5000 PKG used in this experiment.

Figure 3.15 The bomb colorimeter IKA model C 5000 PKG.

7. Scanning Electron Microscope (SEM)

The Scanning Electron Microscope (SEM) is a type of electron microscope that produce image of the sample's surface by scanning of focus beam electrons. The coating of samples is necessary before examination in the SEM. The creating conductive layer of metal on the sample helps to inhibit charging, reduce thermal damage and improve the imaging of sample. The samples were coated thin gold layer on sample's surface before scanning by SEM. Figure 3.16 shows SEM (model of JEOL JSM 6010LV) used in this experiment. The scanning condition are mode SEI, SS40, Accelerating Voltage(ACC) 10-15 kV, Working Distance (WD) around 30 mm.

Figure 3.16 The Scanning Electron Microscope (SEM) model JEOL JSM 6010LV

8. Thermogravimetric analysis (TGA)

Thermogravimetric analysis (TGA) is a method of thermal analysis used to examine the weight change that occur as the sample was heated at constant rate. The dried yeast and biochar were measured percent of moisture, volatile matter, ash, and

fixed carbon in the sample by monitoring the weight change. The TGA model of LECO

701 was used to determine biochar's thermal stability as shown in Figure 3.17
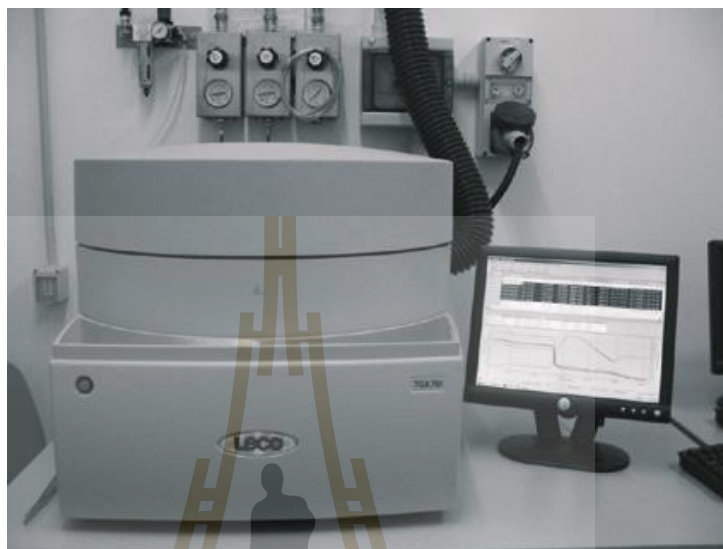
Figure 3.17 The TGA machine model of LECO 701.

9. X-Ray Diffractometer (XRD) Analysis

X-Ray Diffractometer (XRD) is one of microstructural analytical technique

that study the crystal structure. The sample was identified the crystalline phases present

in a material, and thereby reveal chemical composition information. The XRD was used

to investigate biochars, and it was shown in Figure 3.18 (BRUKER D2 PHASER

XRD). It was operated at step time 0.5 and 2θ of range 10-80⁰.

Figure 3.18 BRUKER D2 PHASER XRD.

10. Fourier-transform infrared spectroscopy (FTIR)

Fourier Transform-Infrared Spectroscopy (FTIR) is an analytical technique used to identify organic (and in some cases inorganic) materials. This technique measures the absorption of infrared radiation by the sample material versus wavelength. The infrared absorption bands identify molecular components and structures. The obtained biochar was analyzed functional group by using FTIR model BRUKER(TENSOR 27-Hyperion) as shown in Figure 3.19

Figure 3.19 FTIR model BRUKER (TENSOR 27-Hyperion)

11. The surface area and porosity analysis by BET (Brunauer, Emmett and Teller)

The specific surface area of a sample was determined by BET related to total surface area, porous structure, and pore size distribution. This information was used to predict product characteristics. Furthermore, it is useful in evaluation of product performance and manufacturing consistency.

The Micromeritics ASAP 2020 plus is an advance instrument that combine different automated gas sorption technique into a single. The machine was shown in Figure 3.20 It is designed to provide high-quality surface area, porosity, and chemisorption isotherm data.

The BET instrument applied by Particle Analytical (Micromeritics ASAP 2020 plus) determines the specific surface area (m^2/g) of biochar samples. The samples were dried with nitrogen purging or in a vacuum applying elevated temperatures. The volume of gas adsorbed to the surface of the particles. That was measured at the boiling point of nitrogen (-196 °C). The amount of adsorbed gas was correlated to the total surface area of the particles including pores in the surface. The calculation was based on the BET theory. Traditionally, nitrogen is used as adsorbate gas. Gas adsorption also enables the determination of size and volume distribution of micropores (0.35 – 2.0 nm).

Figure 3.20 The Micromeritics ASAP 2020 plus.
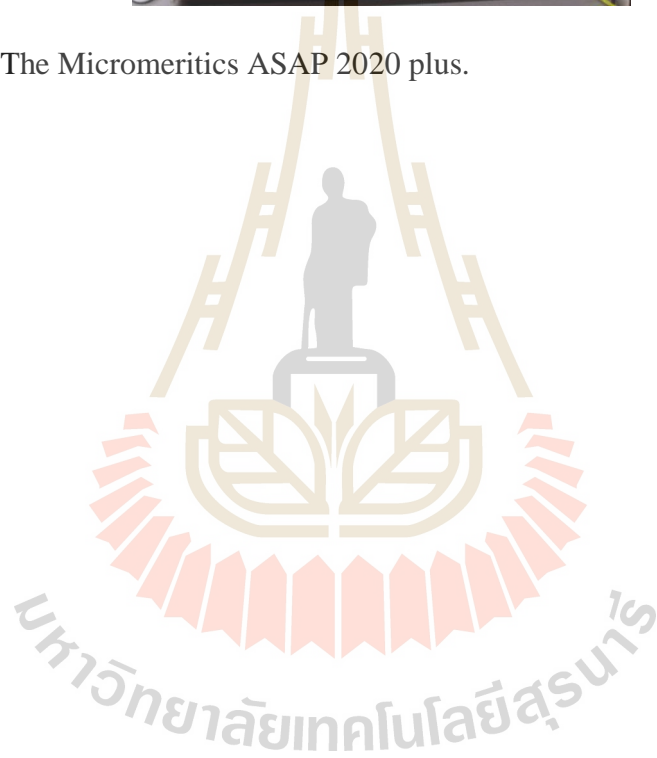
CHAPTER IV

RESULTS AND DISCUSSIONS

4.1. Fermentation of *Rhodosporidium paludigena*

The profiles of oleaginous yeasts depend on the species. and the growth conditions. Environmental conditions include temperature, pH, substrate, C/N ratio and oxygen (Pakawat Kraisintu *et al*., 2010). The profile of oleaginous yeast was shown in Figure 4.1 including cell concentration, glucose concentration, and pH, respectively. The fermentation of *R. paludigena* in working volume of 350 L with an initial pH of 4.66, agitation of 150 rpm at 30 °C. The initial glucose concentration should not be over 80 g/L, it might be error from glucose measurement. This strain gave maximal concentration of 22.42 mg dry cell/mL at 168 hr.
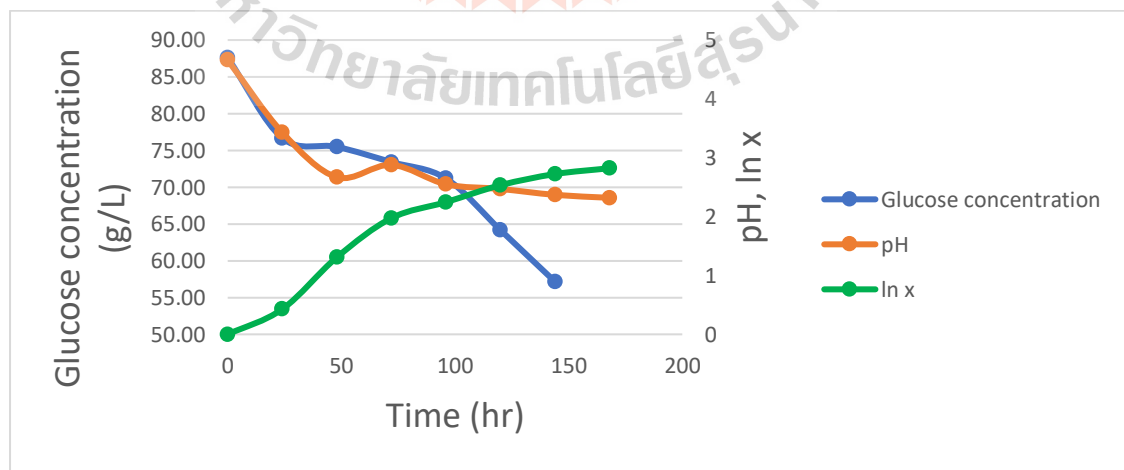
Figure 4.1 Time course of cell concentration(ln x), glucose concentration(mg/mL) and

pH in fermentation of *R. paludigena* in a 500 L bioreactor.

When oleaginous yeast was inoculated into new medium 350 L, cell concentration slightly changed within the period of approximately 24 hr. This was considered as lag phase. After that, cell concentration entered to the exponential phase during 24-72 hr. The slope of growth curve in this period was used to calculated the specific growth rate (μ) of 0.641 day^{-1} resulting in the doubling time (t_d) of 1.08 day as shown in Figure 4.2 It means that the oleaginous yeast *R. Paludigena* took time around 1 day to grew double in the exponential phase. After the third day, the growth of *R. paludigena* began to slow down because the medium and nutrients were depleting and increasing of waste. This period, the growth was in stationary phase.
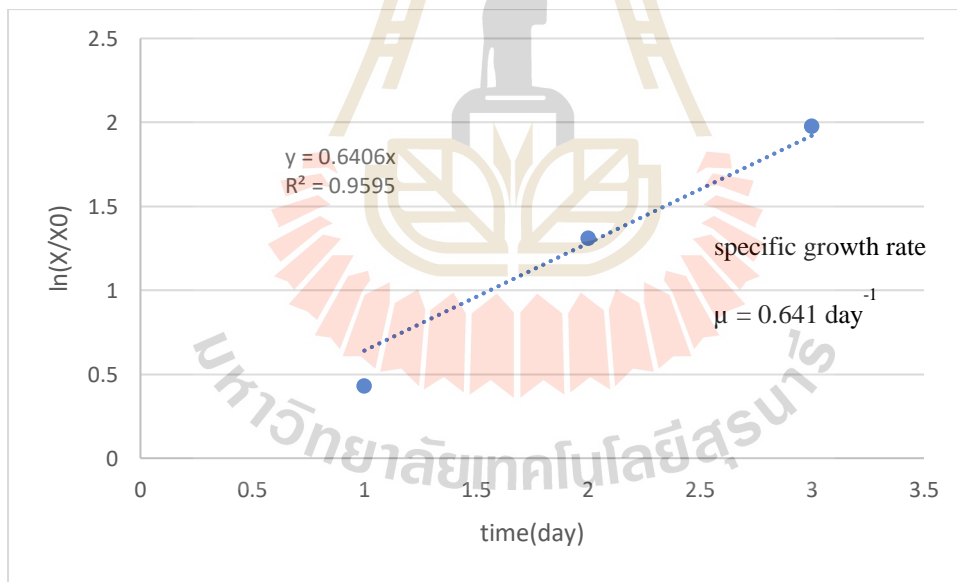
Figure 4.2 Measurement of specific growth rate in exponential phase.

4.2 Cell harvesting

4.2.1 Centrifugation

A disc stack centrifuge was tested for cell recovery of the oleaginous yeast *R. paludigena.* The initial broth fermentation of 5 L with the OD_{600} at 2.06 was fed into the disc stack centrifugation. That results was found light phase of 3500 mL, heavy phase of 700 mL. as shown in Table 2.1.

The highest efficiency of removal of disc stack centrifuge for separation of *R. paludigena* was 95.73 % which was shown in Table 4.2. Although the efficiency of removal of disc stack centrifuge was high and cake from centrifugation was very concentrated that became a slurry, this process was reported that the energy consumption for disc stack centrifuge was higher than the other unit operations (Amaro *et al.,* 2017). In addition, the equipment size was too small to handle with a 350 L of the fermentation broth. As a result, the method was changed to membrane separation.

Table 4.1 Data from a disc stack centrifuge experiment.

Analysis	Results
Initial volume	5000 mL
Final volume	4200 mL
Solid cake	28.4 g
Light phase	3500 mL
Heavy phase (OD_{600} = 1.086)	700 mL
OD_{600} (Stock cell)	2.06

Table 4.2 OD_{600}, cell per volume of light phase, and percent of removal of *R. paludigena*.

time(min)	OD_{600}	percent of removal
5	0.088	95.73
10	0.156	92.43
15	0.115	94.42
20	0.211	89.76
25	0.459	77.72
30	0.464	77.48

4.2.2 Membrane separation

The fermentation broth was filtered through a microfiltration unit to separate yeast cells from fermentation broth. In cross flow experiment, the cell removal rate was of interest. The changing of flux was shown in Figure 4.3. Filtration of *R. paludigena* culture was investigated in an cross-flow micro-filtration system. The membrane with 18 m^2 surface area, and 0.1 μm pore diameter was operated at the trans-membrane pressure of 1 bar. Every 25 or 20 L of the permeate was collected and the time used was recorded. The pure water flux was obtained at a constant value of 105 L/m^2.h. However, a flux decline characteristic was observed with the changing of pure water to fermentation broth. The flux decreased rapidly during the first 500 s followed by a slightly decreased until the end of the experiment. Cells were collected for further downstream processing for spray drying. In addition, a cleaning method was employed to the machine by RO water followed by 1% NaOH. The recovered flux of water was recorded of each cleaning step until it reached to the original flux value.
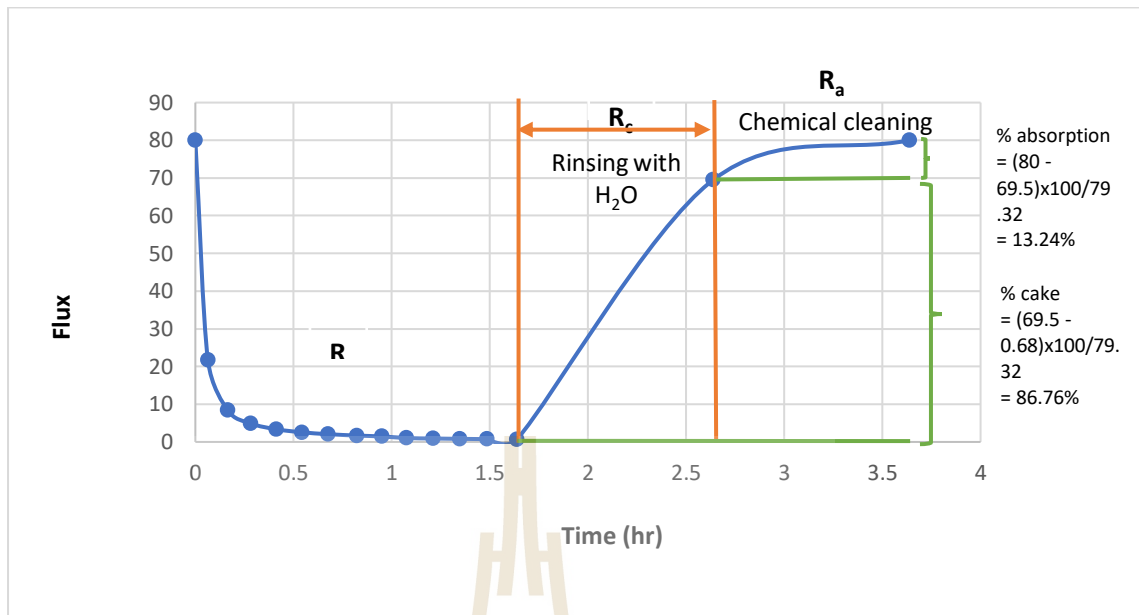
Figure 4.3 Time course of flux in cross flow microfiltration.

In dead-end filtration, the change of flux was shown in Figure 4.3 *R. Paludigena* broth 50 mL was transferred to a dead end filtration test cell. The filter is nylon membrane pore size of 0.1 µm diameter and sure face area of 1.7×10^{-3} m^2. Nitrogen gas was applied to pressurize 1 bar. Every 5 ml of permeate was collect and the used time was recorded.

The permeate flux change could be divided in three periods. An initial period, characterized by a rapid flux decrease attributed mainly to concentration polarization occurring very rapidly, a second period corresponding to a less severe decrease of the flux due to the effect of interactions between the material making up the membrane and the solute, and a third period corresponding to a small flux decreased until a pseudo steady-state was reached(Taherian et al., 2015). The comparison of flux changing curve between dead end and cross flow filtration was presented in figure 4.4 The flux change in dead end rapidly decreased although flux in first stage was very high because the membrane was quickly blocked around VCR of 3 by cake accumulation. While flux of

cross flow membrane was lower in the initial stage and that reached pseudo steady-state until finished.
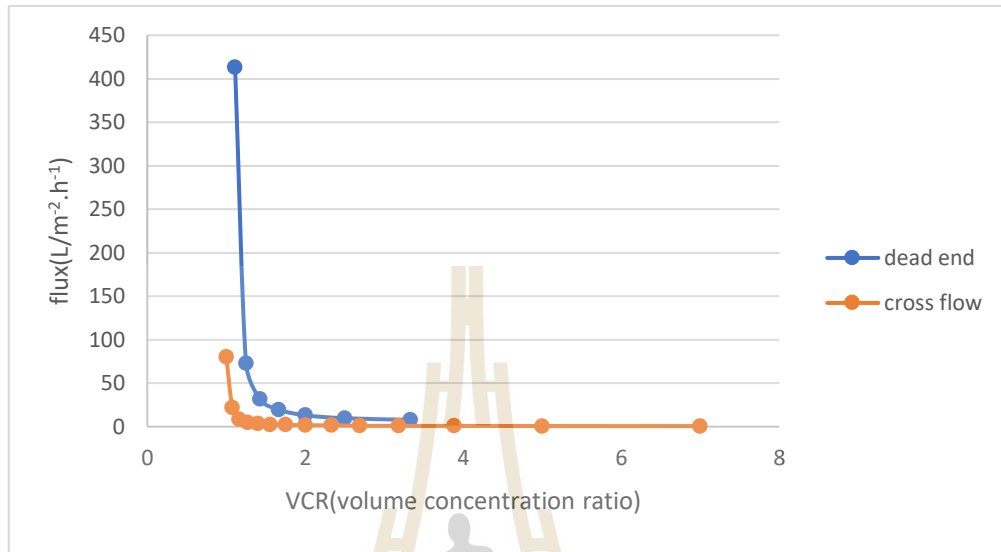
Figure 4.4 The relationship between flux ($L/m^{-2}.h^{-1}$) versus volume concentration ratio(VCR) in dead end and cross flow filtration.

The Darcy'law was applied to solve the total resistance. Which include resistance of membrane and cake. The applied Darcy'law equation shown as follow:

$$\frac{At}{V} = \frac{\mu\alpha p_c}{2\Delta p}\left(\frac{V}{A}\right) + \frac{\mu R_m}{\Delta p}$$

This equation is valid for incompressible cake. It mean cake's compressibility (α) is constant The term (At/V) was plotted versus (V/A) as shown in Figure 4.5 to solve the total resistance (R) containing membrane resistance (R_m) and cake resistance (R_c). The intercept was used to solve R_m and α was determine from the slope assuming that the viscosity of broth (μ) is 10×10^{-3} kg/m·s with the mass of dry cake solids per volume of filtrate (ρ_c) of 22 kg/m^3. As shown in Figure 4.5(a), the plot give R_m= 6.28 $\times 10^{10}$ m^{-1} from intercept, and the α value of 3.63×10^{13} m/kg or R_c=14×10^{12} m^{-1}. Thus, the $R_{dead\ end}$ is around 14×10^{12} m^{-1} in dead end filtration. In Figure 4.5(b) of cross flow

filtration, $R_m = 2.29 \times 10^{12}$ m^{-1} from intercept and α value of 1.09×10^{13} m/kg or $R_c = 4 \times 10^{12}$ m^{-1} was obtained from the slope. As a result, the $R_{cross\,flow}$ is 6.29×10^{12} m^{-1}. The cake resistance of dead end filtration is higher because the cake in dead end filtration was more accumulated at the membrane surface than the cross flow filtration. The cross flow removes the cake layer built up from the surface of the membrane, the permeate flux does not drop as fast in comparison to dead end filtration. However, the membrane resistance of dead end was lower than cross flow filtration because of thickness of membrane and surface area of membrane.
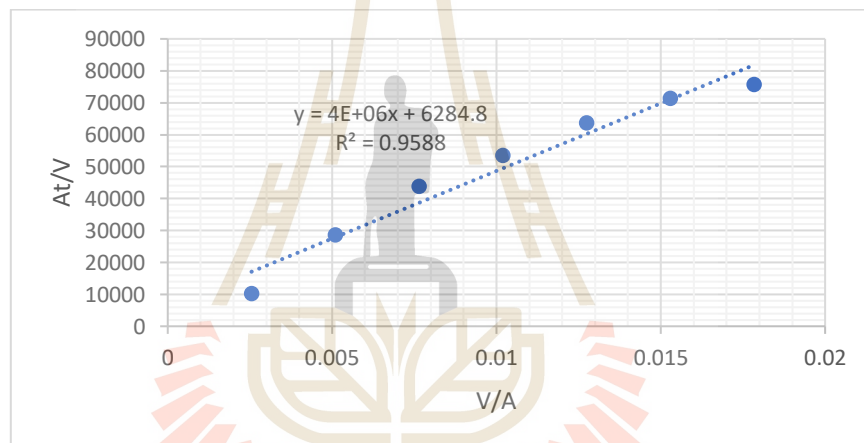
(a)
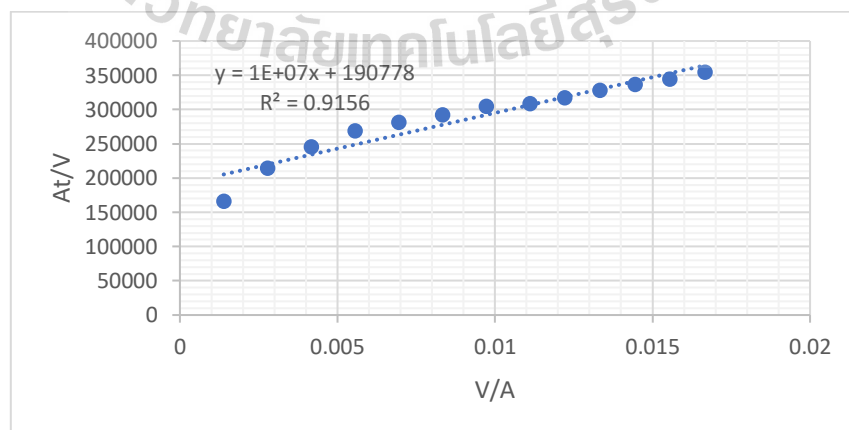
(b)

Figure 4.5 Relationship of (At/V) versus (V/A) as follow applied Darcy's law equation

of filtration of *R. Paludigena* broth in (a) dead end filtration (b) cross flow

filtration. The cake was assumed that is incompressible cake.

Theoretically, the efficiency from filtrated with dead-end should be lower at the

time because of the thicker of cake layer were formed above of membrane. Flux of

samples decreased over time and took around 1.2 hours to get 35 mL of filtrated sample.

While the efficiency of cross-flow filtration should be high in the initial time, and

continuously decreasing until constant. In the other hand, cake forming was increasing,

and stable because of flowing phenomenal was reducing cake thickness. However, 350

L of cross-flow filtration absolutely discord with theory. Apparently, the reason that

made cross-flow filtration became a low efficient came from membrane washing. Both

of percentage cake formation and absorption literally confirm that membrane must be

washing and test the efficiency before applied in industrial. Moreover, there were so

many factors to concern when scaling up to industrial scale. Normally, challenging is

not occurred in downstream processing compare to upstream that have so much factors

to solve. For the water cleaning, the permeate flow rate 1,250 L/h when calculated to

the regained flux after water washing as 69.50 $L/m^2.h$ and the regained flux after

1% NaOH washing as 80.01 L/m^2h. Thus, percentage of absorption as 13.24% and

percentage of cake as 86.76% as shown in Figure 4.3(C). The retained cells accumulated

on the membrane surface in a growing cake layer. The thickness of the cake layer can

be increased, and cause the increasing in resistance to the permeate flow.

4.3 Spray drying

The *R. paludigena* culture broth was dried by using a spray drying technique.

The nozzle size of 1.4 mm and vacuum pressure of -50 mbar was employed. The feed

rate of broth was 3.5 mL/min, air flow rate 473 L/hr was flown through a heater. The moisture content of the powder decreased with increasing inlet temperature of the drying air (Yue SHI *et al.,*2018). Figure 4.6 shows the spray-dried oleaginous yeast *R. Paludigena.* The typical characteristic of this strain was the red color obtained from its prefixed name "*Rhodo-*". During temperature 110-130 °C, the yield of product and the total loss is not different after 110 °C as shown in Figure 4.7 Some product is high accumulate on surface of column before 110 °C because some water was not in time for removal, thus some product was high moisture and easy accumulate on surface of column at lower 110 °C. The maximal product yield is around 66.7 % at temperature of 110 °C.

Figure 4.6 Dried oleaginous yeast.
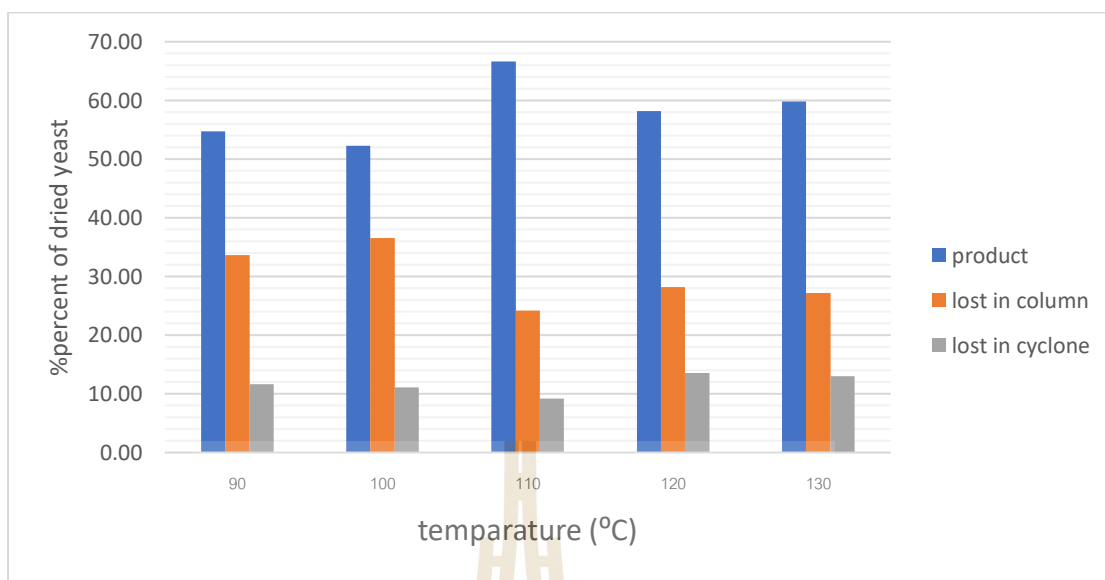
Figure 4.7 The temperature of mini spray drying cell

In general, lipid yield was measured by solvent extraction. Several organic solvents include hexane, ethanol, isopropanol, ethyl acetate, ethyl lactate and etc. These solvents were determined the best solvent for the extraction of yeast oil. Lipid yield in oleaginous yeast *Yarrowia lipolytica*. were reported around 15 % dry weight with no significant difference between hexane and the other solvents. The profile shown that oleic acid (C18:1), linoleic acid (C18:2n6), and palmitic acid (C16:0) were mainly fatty acid in oleaginous yeast (Breil C. *et al*.,2016). In this experiment, petroleum ether was used for lipid extraction of dried sample. The total lipid yield was measured of 19.24 % dry weight. The major fatty acids were around 50 % of oleic acid (C18:1n9c), 20% of palmitic acid(C16:0), 10% of Stearic acid (C18:0), and 10% of Heptadecanoic acid (C17:0) as shown in Figure 4.8
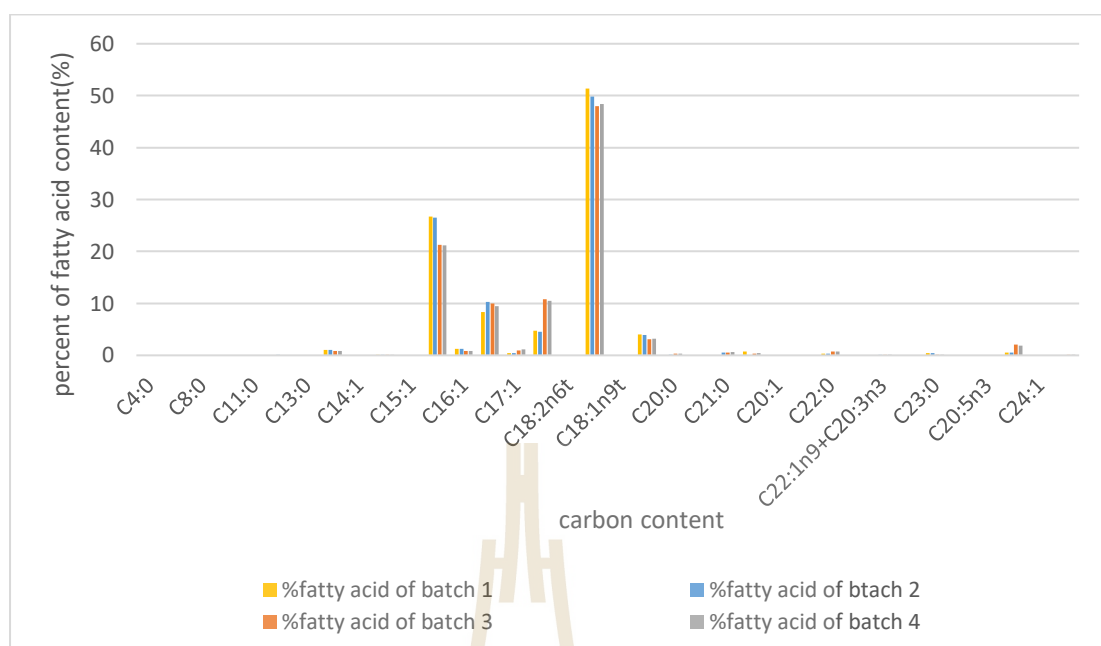
Figure 4.8 Fatty acid of dried oleaginous yeast

4.4 Fast pyrolysis

In fast pyrolysis, biomass decomposed to produce vapors and some charcoal. The vapor was condensed into a dark brown liquid. Rapid cooling of the pyrolysis vapor to give the bio-oil product and some charcoal called "biochar". The biogas is gas that can be not condensed. Fast pyrolysis process carefully controlled operating parameters to give high yields of liquid. The essential features of a fast pyrolysis process for producing liquids include that very high heating and heat transfer rates at the reaction interface, which usually requires a finely ground biomass feed, carefully controlled pyrolysis reaction temperature of around 500 °C and vapor phase temperature of 400-450 °C, short vapor residence times of typically less than 2 seconds and condensation or cooling of fast pyrolysis product (Bridgwater, 2004). The maximum bio-oil yield of azolla, sargassum tenerrimum and water hyacinth were reported (38.5, 43.4 and 24.6

wt.% respectively) obtained at 400, 450 and 400 °C (Biswas *et al*., 2017). The sugarcane bagasse was used as raw material in fast pyrolysis process, the high bio-oil yield was 50.89% that has been obtained at 480 °C. (Al Arni, 2018). Moreover; triglyceride material was investigated for fast pyrolysis process such as the soybean oil with different amounts of double bonds in the chain. The yield was reported around 61-68% at 525 °C and increased with higher amounts of hydrogenated fat or saturated fatty acid in the sample (Beims *et al*., 2018). The bio-oil was showed in Figure 4.9(a). The colour of bio-oil is like petroleum. The biochar was removed out from fixed bed fast pyrolysis reactor. Figure 4.9(b) shows the biochar obtained from fast pyrolysis process. The maximum bio-oil yield of dried oleaginous yeast *R. paludigena* was obtained 60 wt% at 550 °C as shown in Figure 4.10 The different physical and chemical properties of raw materials affected significantly to yield and characteristic of bio-oil by decomposition and multiple complex reaction. For improvement, the fast pyrolysis process, heat transfer and mass transfer could be increased by using a continuous reactor but feeder of continuous reactor can be blocked by packing of dried yeast powder. The reactor could be modified with spray dryer by addition atomizer into fast pyrolysis reactor. but bio oil might contain high water and that could be upgraded by water adsorption.

Normally, a few biogas was obtained in fast pyrolysis process. The dry wood was passed fast pyrolysis process, the biogas yield was reported around 13 % (Bridgwater, 2004). The microalgae strain of Chlorella vulgaris was pyrolyzed by using a fluidized bed reactor at a temperature of 500 ⁰C, biogas yield was reported 10 % (Krishnakumar et al., 2016). Biogas in this work was around 20 %, that was higher than because condensable gas could be not trapped.

(a)   (b)
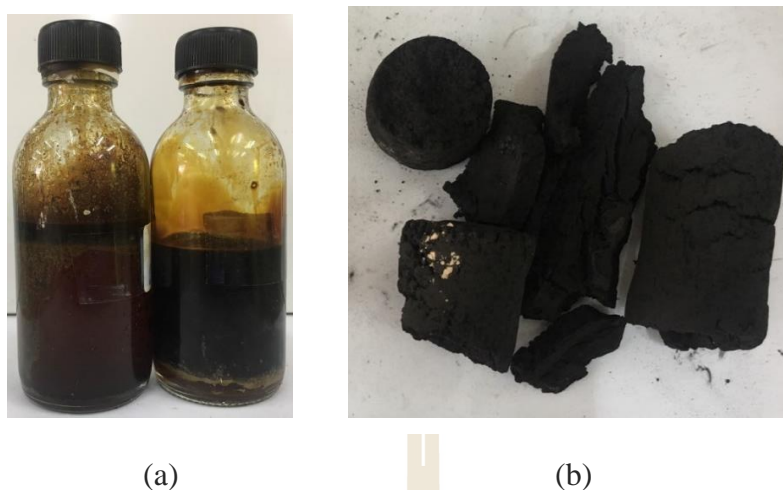
Figure 4.9 The bio-oil (a) and biochar (b) from oleaginous yeast *R. Paludigena.*
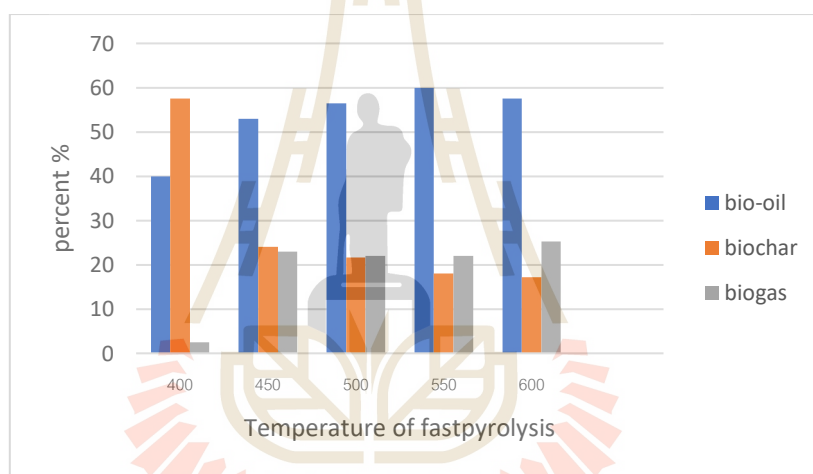
Figure 4.10 Percent yield of bio-oil, biochar and biogas.

4.5 Bio-oil characterization

The compounds group and amount of frequency of carbon group in the bio-oils according to the number of carbon atoms in the chain are shown in Figure 4.11 The most frequency of compounds was in the range of C5 to C11 as shown in Figure 4.11(A). The volume of compound groups composed range of C16 to C18, and light hydrocarbon(<C8) was shown in Figure 4.11(B). The main fatty acid in oleaginous yeast was decomposed into randomly shorten chain hydrocarbon. Although the cracking fatty acid increased with rising of temperature, the bio-oil yield might be

decreased because when some product was broken down into non-condensable gas or condensable gas could be not trapped.

(A)

(B)
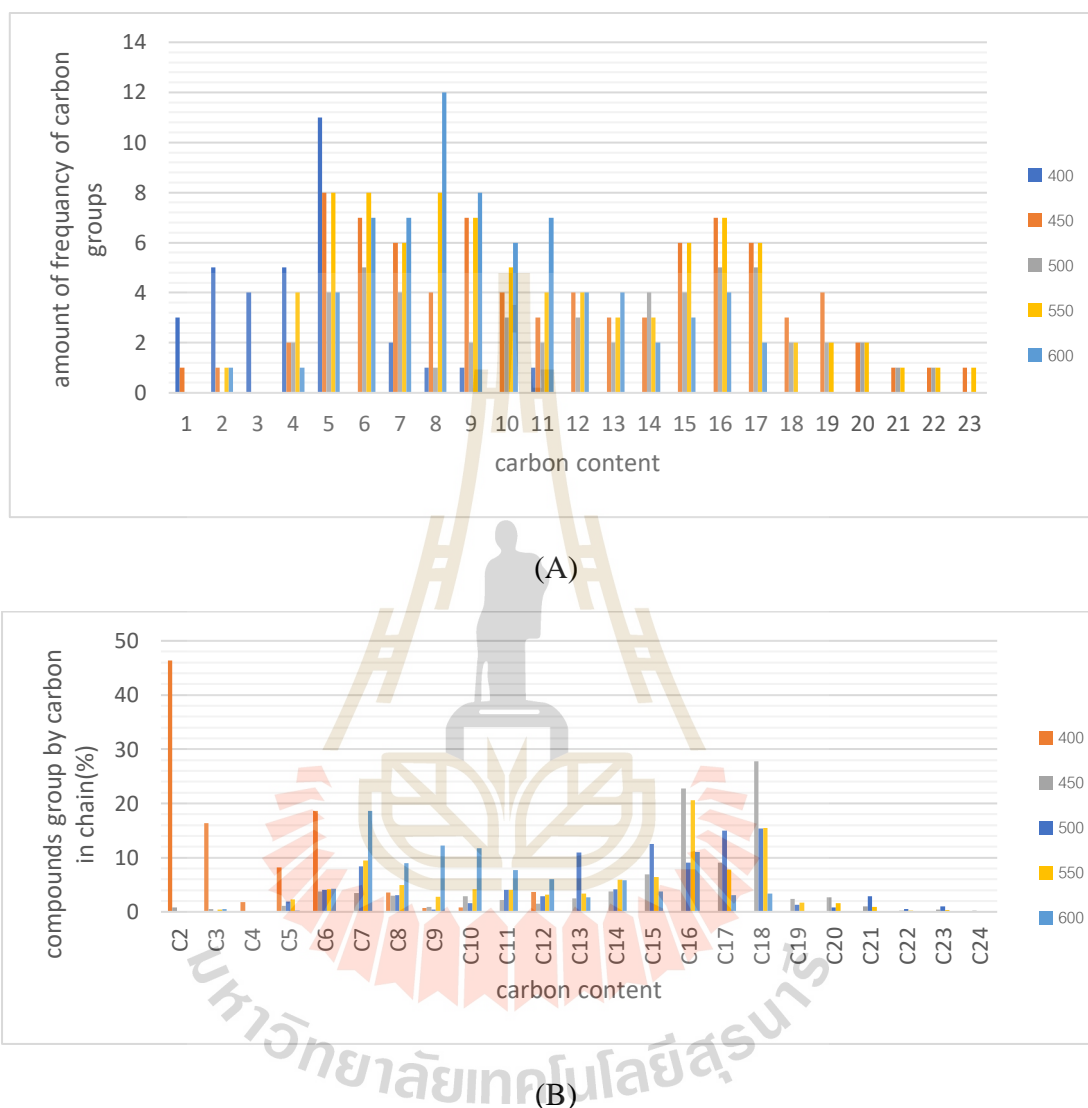
Figure 4.11 Distribution of compounds in bio-oils according to carbon number (A) amount of frequency of carbon group, (B) compounds group by carbon in chain(%V)

The high heating value (HHV) of bio-oil was measured by bomb calories meter as illustrated in Table 4.3. The experimental results showed that the HHV of bio-oil was obtained at approximately 36 MJ/kg. The result was not different significantly. The standard HHV of crude petroleum and biodiesel were 45.543, 40.168 MJ/kg

respectively (www.essom.com). The comparison of crude bio-oil and crude petroleum, the HHV of crude bio-oil was lower than a little because crude bio-oil contained some water higher than standard crude petroleum. The HHV of distillated product was nearly with standard biodiesel. In this work, the elemental content and water content of bio oil should be measured.

Table 4.3 High heating value (MJ/kg) of each condition of bio-oil.

Bio-oil	high heating value (MJ/kg)
400 °C	-
450 °C	36.420
500 °C	36.123
550 °C	35.872
600 °C	35.703
Distilled fraction (Short path distillation)	37.511
Stillage	34.946

4.6 Biochar characterization

Unsaturated chains tend to favor the cracking reaction between the double bonds and subsequent bond cleavage into smaller molecules, which may also lead to form coke. The yield of biochars from thermal cracking of soybean oil and blends with hydrogenated fat were presented around 9.7-15.0% at 525 °C (Beims *et al.,* 2018). In this work. the yield of biochar decreased from 66.56 to 24.46% with the increased pyrolysis temperature from 350 to 550 °C. The consequence was because the primary thermal degradation of biomass occured at lower temperature. After that, subsequent increased in the temperature further crack the volatile materials into low-molecular weight organic compounds and gases rather than biochar (Chowdhury *et al*., 2016). The

highest biochar yield of this work was 57.5 % at 400 °C. The biochars were measured for carbon, nitrogen, hydrogen and oxygen content. The element of biochar was analyzed, and was reported range of elemental proportions C (30.7–78.5%), N (0.49–2.54%), O (7.9–28.0%), and H (0.76–4.01%) (Bird *et al.,* 2017). The elemental content of biochars in this work were measured in the range of C (57.72–65.80%), N (2.66-5.94%), O (9.03-18.77%), and H (2.57-6.53%), respectively as shown in Table 4.2. Carbon and hydrogen content decreased with rising of temperature because Carbon and hydrogen might be removed by decarbonylation and dehydrogenation at high temperature. Nitrogen content was obtained decomposition of protein. Nitrogen content of biochar in this work was higher than other biochar because this yeast might be high protein in cell. The biochemical properties of oleaginous yeast could be improved by genetic engineering. In this work, the elemental content of dried yeast should be measured.

Moreover, the values for ash, volatile matters and the fixed carbon contents were determined as shown in Table 4.4. According to the Japanese standard, the values for ash, volatile matters and the fixed carbon contents of briquettes are from 3% − 6%, 15% - 30%, and 60% − 80 %, respectively (Lestari *et al.*, 2017). Although the values for ash content and volatile matter of biochars at 400-450 °C exceeded the standard value, but for volatile matter of biochars at 500-600 °C and fixed carbon contents are in good agreement with the standard. The volatile matter in biochar was significantly decreased with rising of temperature because the volatile matter was removed during decomposition. The increase of ash content brings disadvantage in biochar application because the ash tends to increase the pollution and dust.

Table 4.4 Elemental (C H N O) contents, the values for ash, volatile matters, the fixed

carbon contents and moisture of biochar in this work.

biochar	%C	%H	%N	%O	Ash	volatile	Fixed carbon	moisture
400°C	65.80	6.53	2.66	9.03	15.99	51.13	31.09	1.79
450°C	65.47	5.55	4.38	7.63	16.97	33.74	47.00	2.29
500°C	63.29	3.46	5.94	18.77	8.54	22.92	63.19	5.34
550°C	61.46	3.12	4.50	9.58	21.34	17.30	56.95	4.41
600°C	57.72	2.57	3.14	9.24	27.33	19.58	49.10	3.99

The comparison between HHV of biochar at 400-600 °C (Table 4.5.) with standard coal (www.essom.com) were found that HHV of biochar at 400-500 °C were nearly with bituminous coal (27.267 MJ/kg)**.** The HHV of other biochar (550-600 °C) and dried oleaginous yeast were nearly coal or sub bituminous (23.968 MJ/kg). In theory, the bituminous included carbon content higher than sub bituminous. Consequently, the heating value of biochar was significantly increased with rising of carbon content.

Table 4.5 High heating value (MJ/kg) of each condition of biochar.

Biochar	high heating value (MJ/kg)
400 °C	28.789
450 °C	27.875
500 °C	27.678
550 °C	24.291
600 °C	21.756
oleaginous yeast	23.174

The scanning electron microscopy (SEM) imagines of biomass and biochar were shown in Figure 4.12 The surface structure of biochar were observed that

increasing temperature from 400 to 600 °C. The biochar was blocked by deposition of ash residues. Normally, biochar was produced by slow pyrolysis. For example, Durian wood (Durio zibethinus) sawdust was used through a fixed bed reactor under an oxygen-free atmosphere at different pyrolysis temperatures (350, 450, and 550 °C). It was reported that the BET surface area increased from 2.567 to 220.989 m^2/g when the pyrolysis temperature increased from 350 to 550 °C (Chowdhury *et al.,* 2016). The BET results, the specific surface area of the material increased from 4.739 m^2/g to 462.826 m^2/g with increasing pyrolysis temperature (Liu *et al*., 2020). In this work, the results were shown in Table 4.6. the BET surface area range of 2.619 to 8.370 m^2/g, external surface of 2.464 to 7.592 m^2/g, total pore of 0.915 to 3.598 mm^3/g, and the average pore diameter of 62.176 to 187.642 Å, respectively.
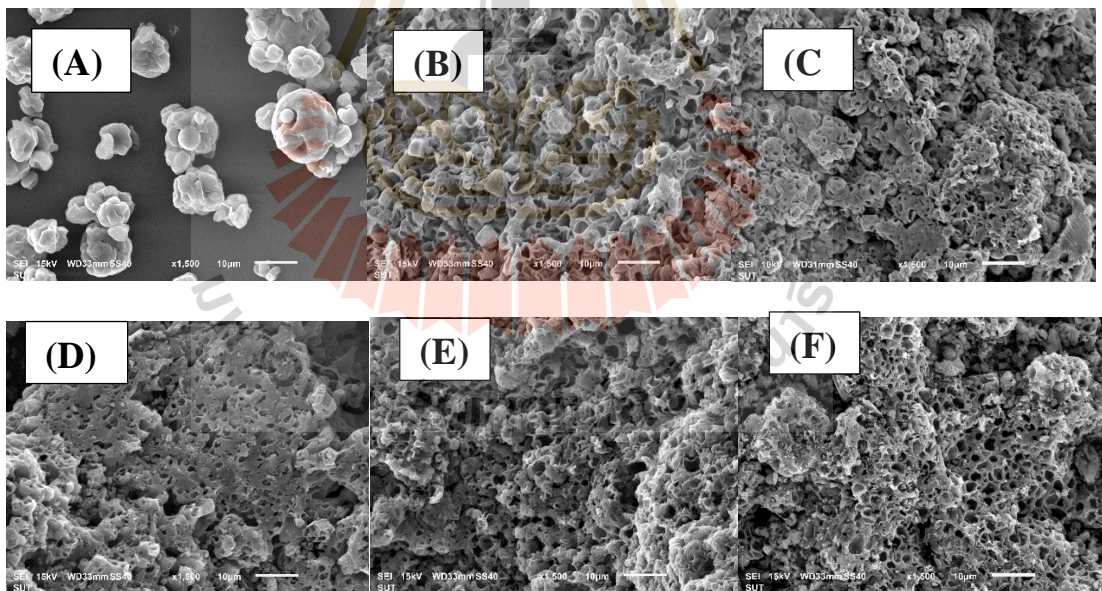

Figure 4.12 SEM imagines of biomass and biochar: (A) dried oleaginous yeast; (B) biochar 400 °C; (C) biochar 450 °C; (D) biochar 500 °C; (E) biochar 550 °C; (F) biochar 600 °C (SEI, SS40, 15.0 kV).

Table 4.6 BET surface area analysis of biochars.

| biochar	BET surface area (m^2/g)	External surface (m^2/g)	Total pore (mm^3/g)	Average pore diameter (Å)
400 °C	4.089	6.337	1.207	62.176
450 °C	2.628	3.788	0.915	110.097
500 °C	4.961	4.241	2.161	125.555
550 °C	2.619	2.464	1.095	187.642
600 °C	8.370	7.592	3.598	130.670

The XRD patterns for biochar was shown in Figure 4.13 The structure and chemical compositions of biochar were depicted by identification of peaks from XRD. The strong peaks were found at range of 2θ=25-45º. The XRD spectral analysis of biochar produced at 250–450 °C showed various peaks for example biochar at 250 °C, and found the strong peak at 2θ=28.3º, 26.5º and 31.4º showing the presence of fluorite, graphite, and chlorapatite. At 450 °C, the prominent sharp peak at 28.39° showed the presence of fluorite, while other high-intensity peaks at 31.41°and 40.36°were assigned to chlorite and gibbsite. In addition to these strong peaks, many other medium intensity peaks at 26.56°, 20.88° and 45.34° (2θ) showed the presence of graphite, coquimbite, and hydrobiotite (Waqas *et al.,* 2017). In this work, the strongest peaks of biochar 400 and 600 °C were found at 2θ≈31.5º that possibly showed the presence of chlorapatite. The strongest peaks of biochar 450 and 550 °C were determined at 2θ≈28.5º that might be fluorite. Although peak of biochar 500 °C disappeared, the other peaks were detected at 2θ≈26.5º, 41.0º, 45.0º that possibly were graphite, gibbsite, and hydrobiotite

(A)

(B)
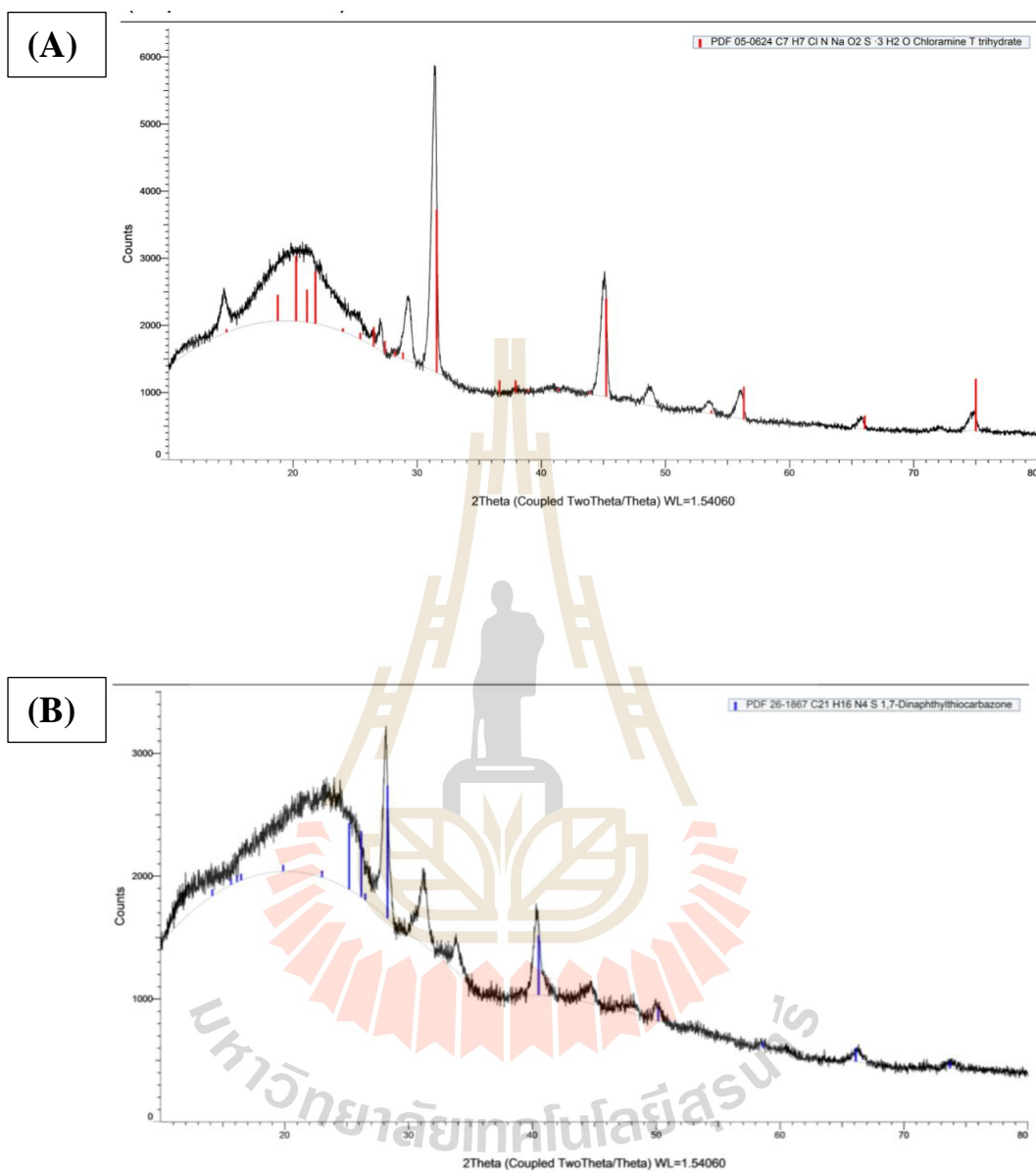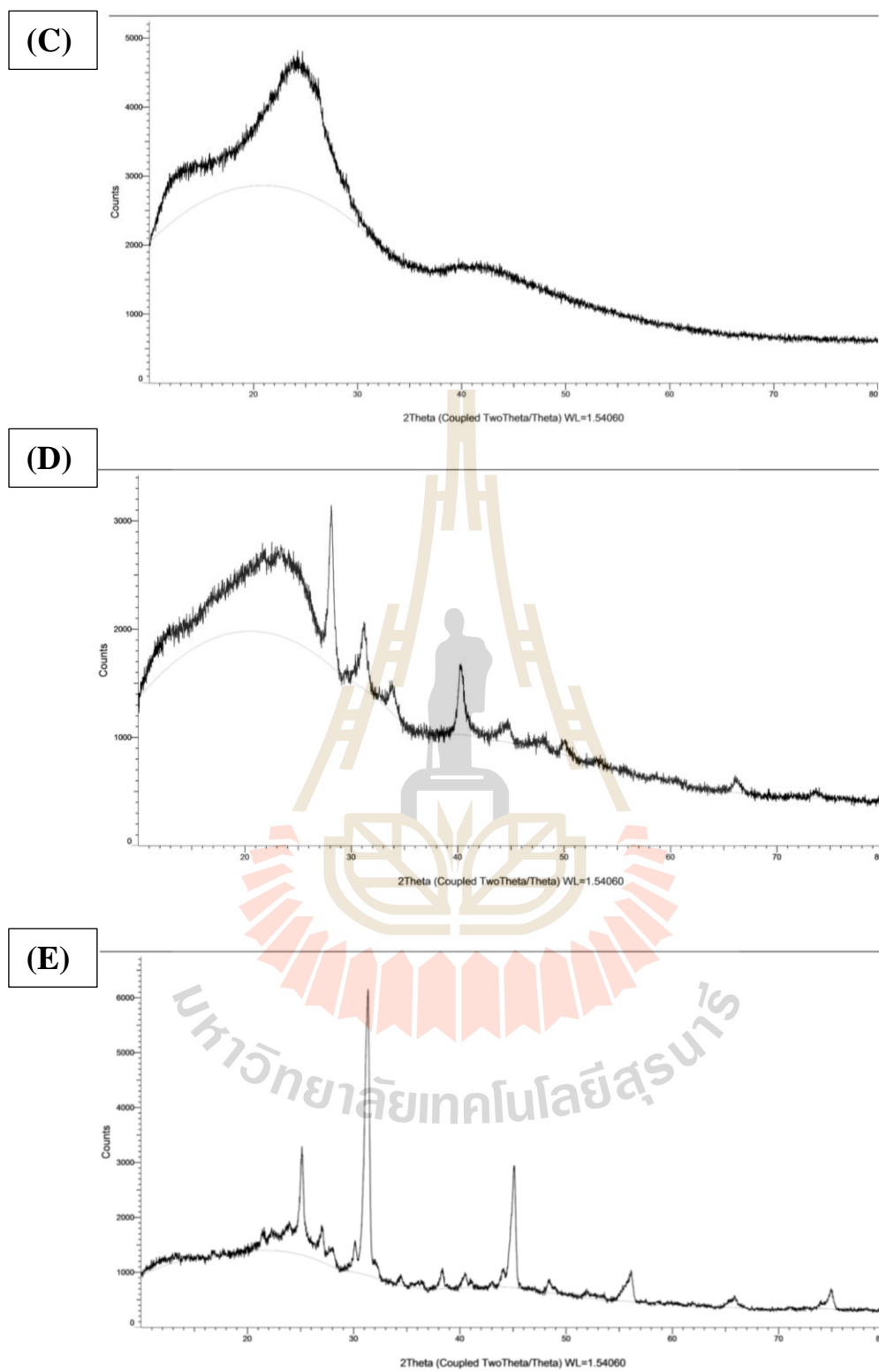
Figure 4.13 X-ray diffractogram (XRD) of biochars :(A) biochar 400 °C; (B) biochar

450 °C; (C) biochar 500 °C; (D) biochar 550 °C; (E) biochar 600 °C

In addition, the biochar were analyzed by FTIR. The FTIR spectrum was given in Figure 4.14, and Table 4.7 lists the functional groups presented in the biochar samples at different pyrolysis temperatures. The peaks in the range of 592 to 646 cm^{-1} were assigned to alkane group (C-H). The peak around 675 cm^{-1} was due to the cis-disubstituted alkenes groups (C=C). The peak in range 721 to 752 cm^{-1}, and 869 cm^{-1} to 860 cm^{-1} were ascribed to the aromatic Benzene (C-H). The peak around 1050 cm^{-1} and 1150 cm^{-1} were due to the alcohol (C-O). The ethers groups (C-O) was about 1100 cm^{-1}. The peak at 1248 cm^{-1} might be ethers or carboxylic acid. The peak around 1380 cm^{-1} were assigned to methyl group (C-H3). The peaks in the range around 1450 cm^{-1} and 1580 cm^{-1} were ascribed as the aromatic ring. The peak at 2293 cm^{-1} to 2322 cm^{-1} might be nitriles groups (C≡N) (https://en.wikipedia.org/wiki/Infrared_spectroscopy_correlation_table). The results were reported that peak at 2920 cm^{-1} and 2851 cm^{-1} were attributed to the presence of methylene group (CH$_2$) (Xu *et al*., 2018).
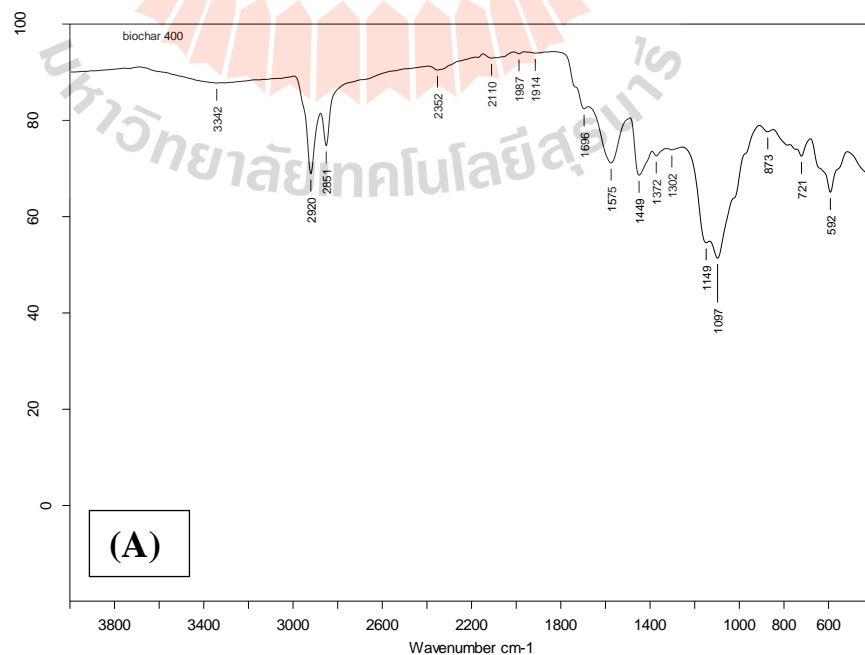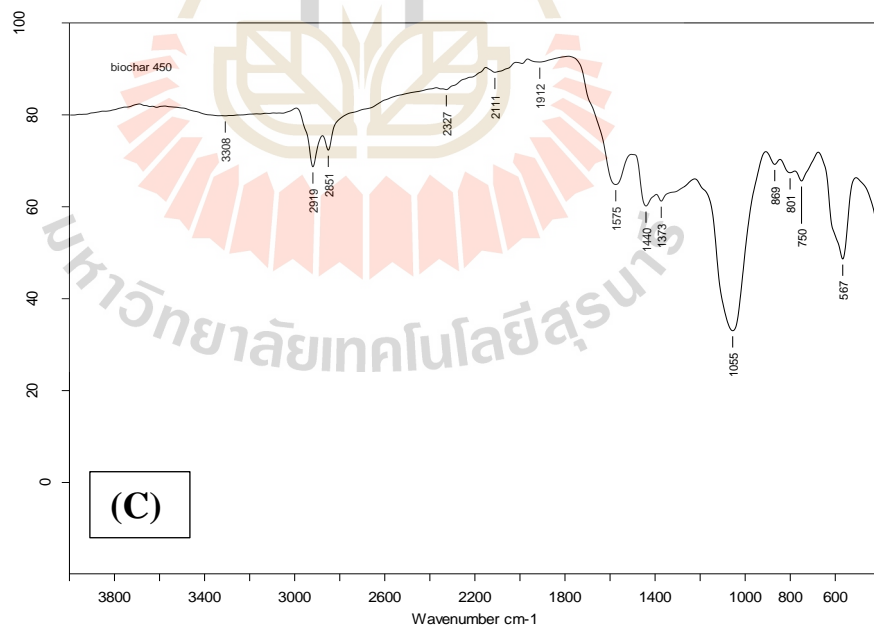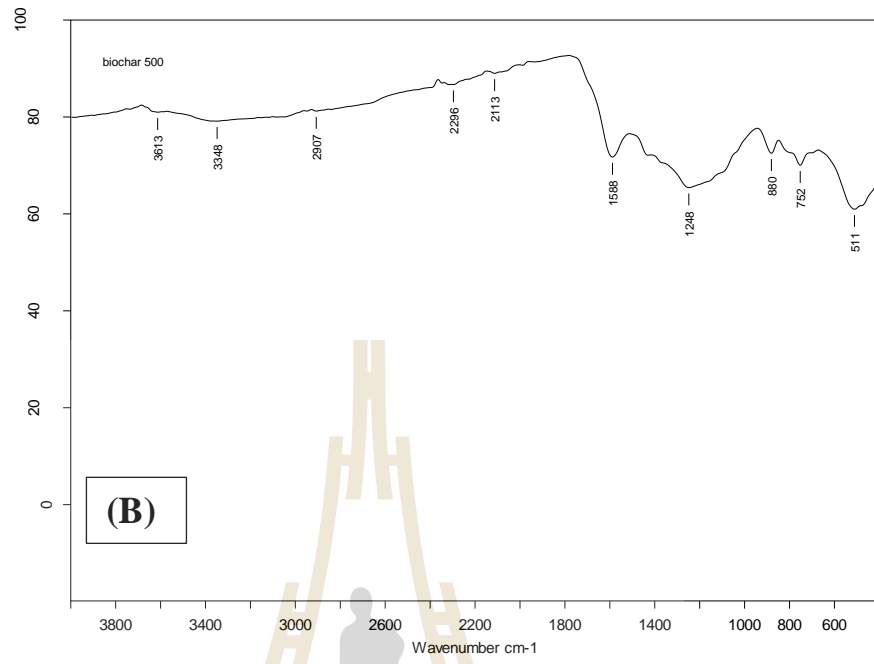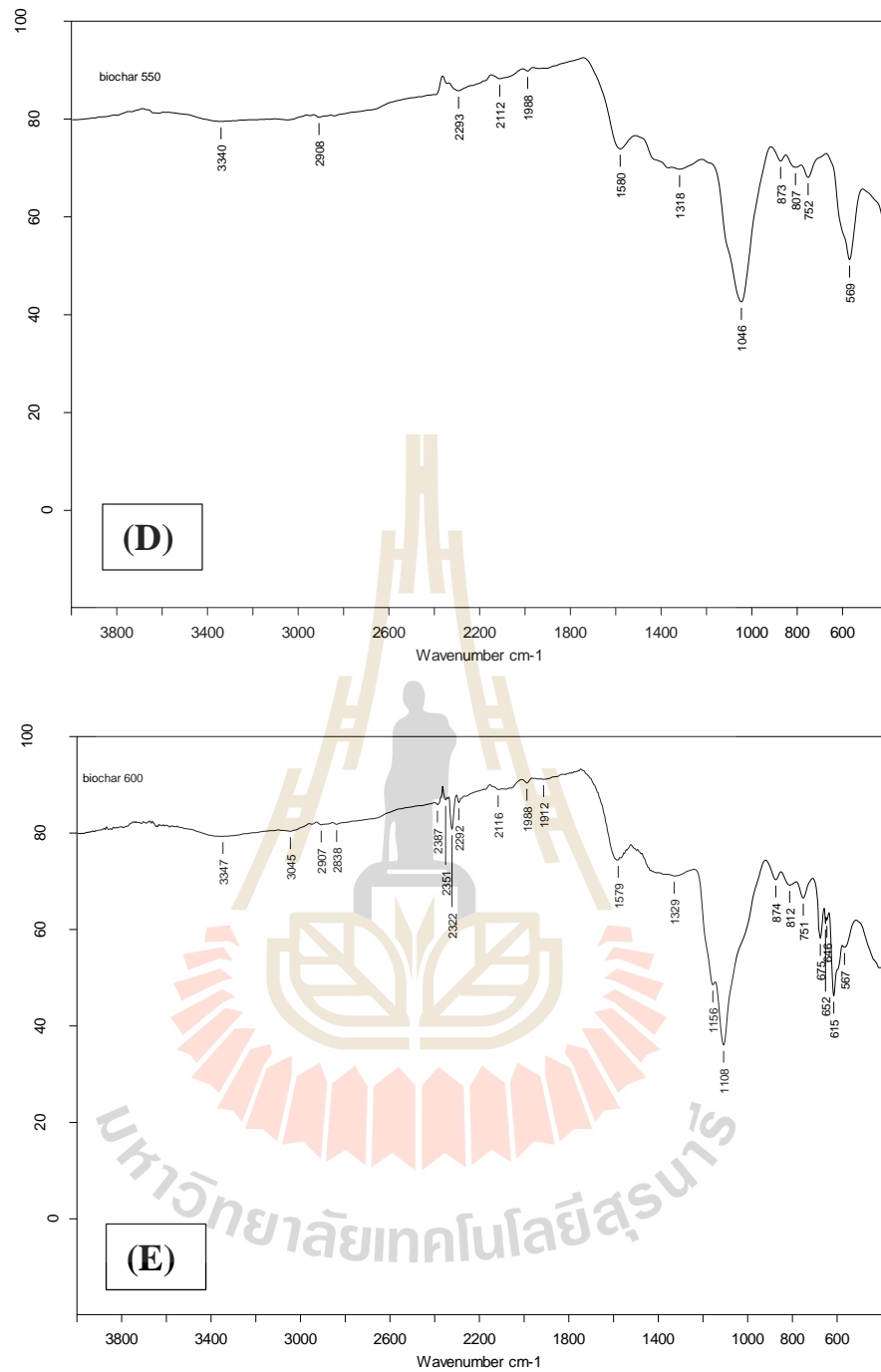
Figure 4.14 The FTIR spectrum biochar:(A) biochar 400 °C; (B) biochar 450 °C; (C)

biochar 500 °C; (D) biochar 550 °C; (E) biochar 600 °C.

Table 4.7 Functional Groups of Biochar Samples Determined by the FTIR Analysis

Specific type of bond	frequency				
	biochar 400°C	biochar 450°C	biochar 500°C	biochar 550°C	biochar 600°C
alkane	592	567	551	569	-
alkane	-	-	-	-	615
alkane	-	-	-	-	646
cis-disubstituted alkenes	-	-	-	-	675
C-H aromatic ortho-disub. benzene	721	750	752	752	751
C-H aromatic para-disub. benzene or trisubstituted alkenes	-	-	-	807	812
C-H aromatic meta-disub benzene	873	869	880	873	874
C-O alcohol	-	1055	-	1046	
C-O esters	1097	-	-	-	1108
C-O alcohol	1149	-	-	-	-
C-O ethers, aromatic or carboxylic acid	-	-	1248	-	-
C-H3 methyl	1372	1373	-	-	-
aromatic C=C	1449	1440	-	-	
aromatic C=C	1575	1575	1588	1580	1579
C≡N nitriles	-	-	-	2293	2322
methylene	2851	2851	-	-	-
methylene	2920	2919	-	-	-

4.7 Short path distillation and SDGC

The Characterization of the C7 to C40 fraction of petroleum crude oils was applied of the simulated distillation technique shortens the time required for characterization from days to hours (Chorn, 1984). The content of crude bio-oil from optimal fast pyrolysis process at 550 ⁰C was identified by simulated distillation gas chromatography (SDGC). The boiling point range of fuels were approximated by heavy naphtha(98-170 ⁰C), kerosene(170-250 ⁰C), biodiesel(250-350 ⁰C) and fuel oil(350⁰C up). The distillation curve of crude bio-oil was shown in figure 4.15(A). The content of crude bio-oil was presented in Figure 4.16 that was determined heavy naphtha of 2.6 %, kerosene of 20.7 %, biodiesel of 24.3 % and fuel oil of 52.4 %. The heavy naphtha was very low, it might be that heavy naphtha not could be trapped by condenser and ESP. The molecular (short path) distillation apparatus was used to separate bio-oil, which came from fast pyrolysis of sawdust at temperature 550 °C and bio-oil yield of 50.39 %. The maximal distillates yield of 85 % at 130 °C, 60 Pa (Wang *et al.,* 2009). The distillate was obtained from short path distillation (SPD) at 150 °C, 10 mbar. The distillates include fraction1 and fraction2, the distillation curve of distillates and stillage were shown in figure 4.15(B), (C) and (D). The distillates yield was around 49 % as appearance in figure 4.17 Each fraction were measured by SDGC. The result was shown in Figure 4.18, biodiesel were determined fraction1 of 32 %, fraction2 of 37.6 % and fraction3 of 5.4 %. The fuel oil were measured in fraction1 of 14.4 %, fraction2 of 51.3 %, and fraction3 of 92.3 %. Although the highest kerosene was found in fraction1 around 53.4 % but yield of fraction1 was vary low. A few kerosene was found in fraction2 of 10.6 % and fraction3 of 1.5 %, respectively. Thus, this condition was not suitable to produce kerosene. Although fuel oil in fraction 3 was very high, it could be

improved by catalytic cracking for example heavy oil was upgraded by using TiO2 and ZrO2 catalysts in fixed bed reactor, the heavy oil was converted to lighter fuel under superheated steam conditions (Kondoh et al., 2016).
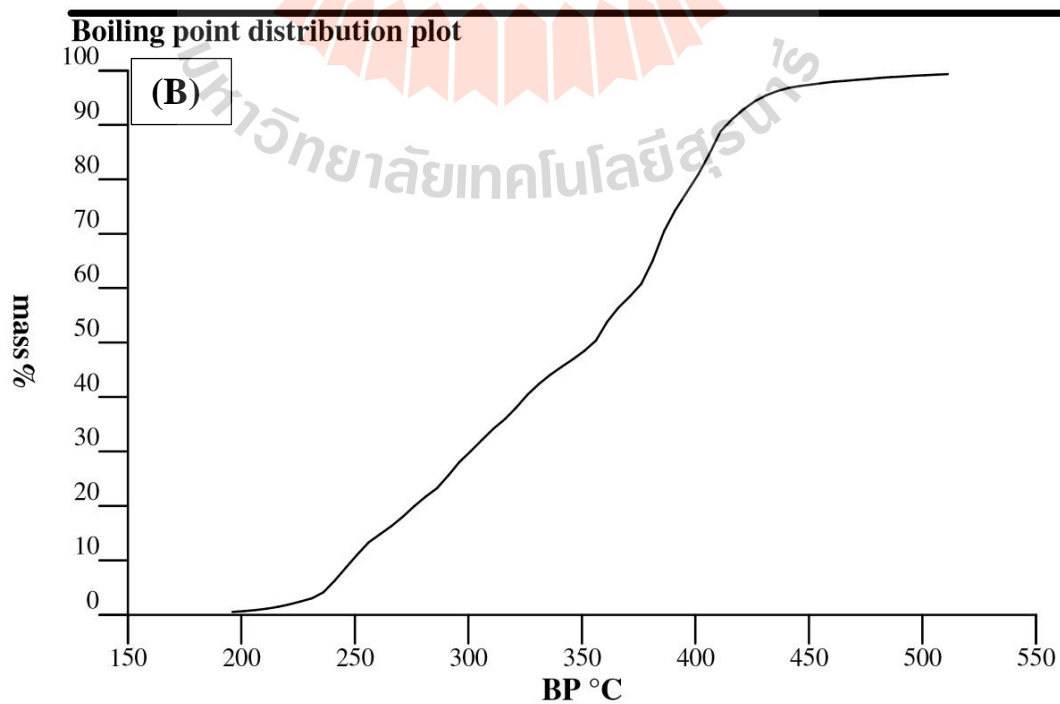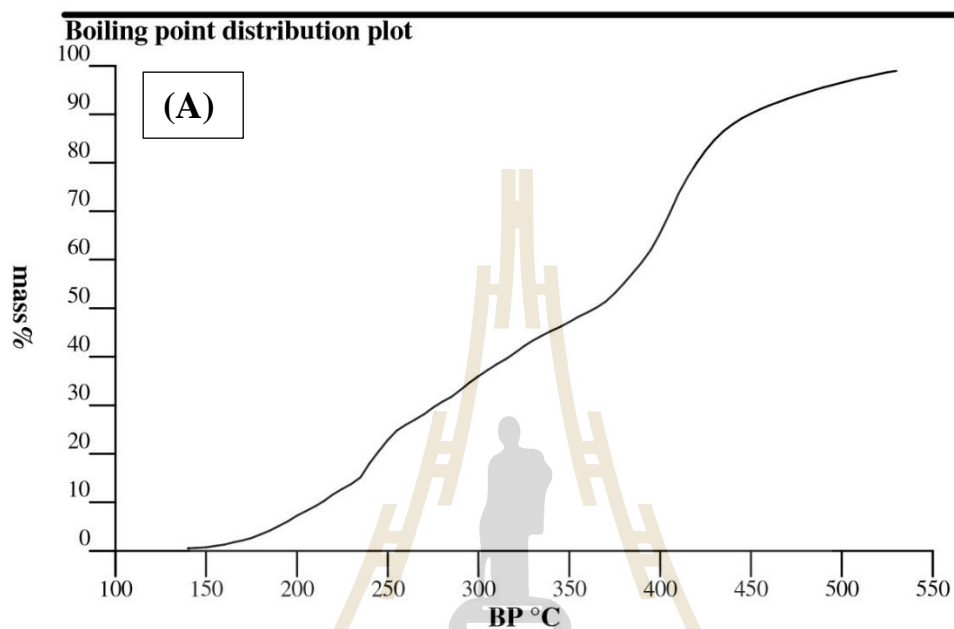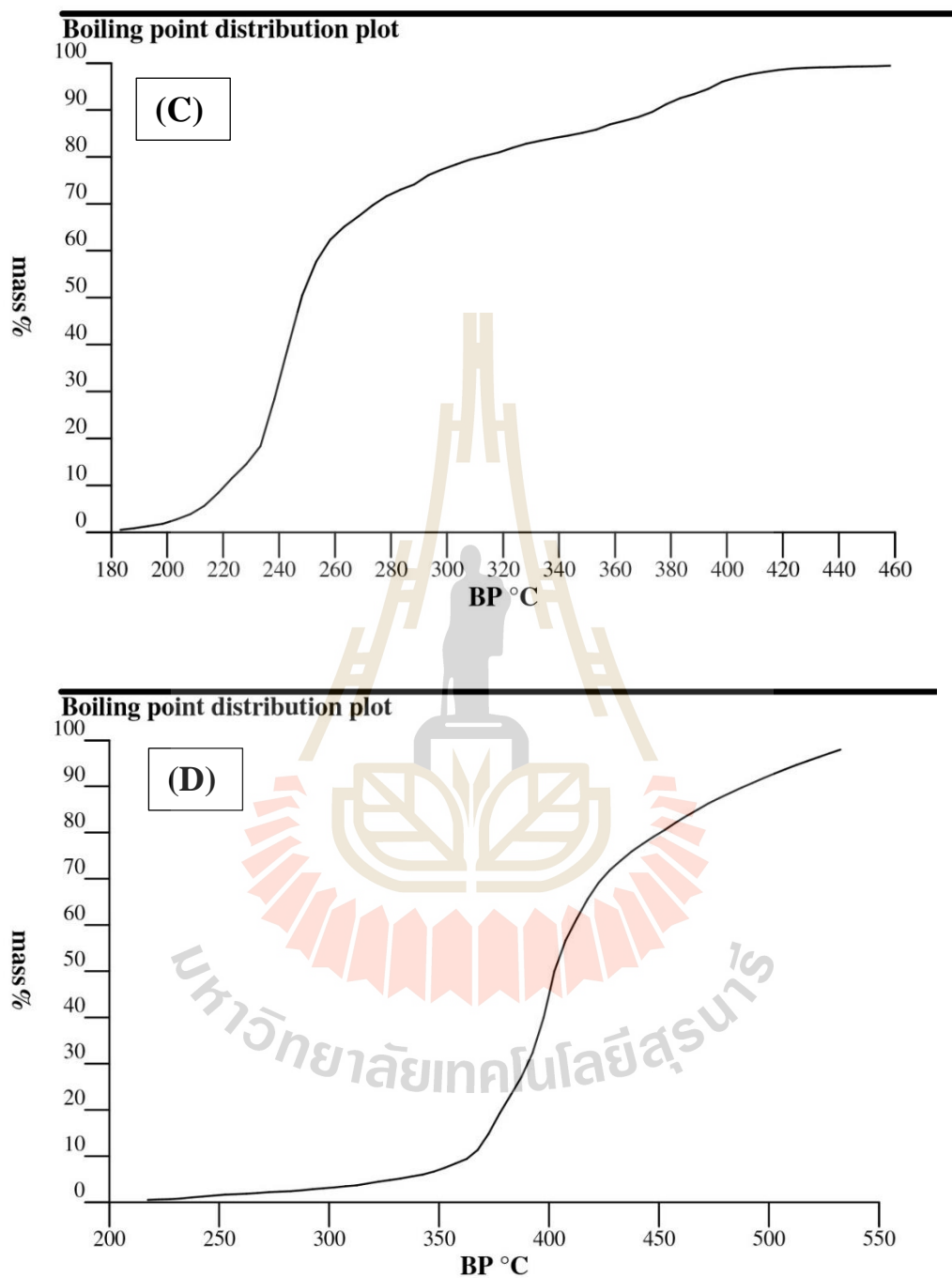
Figure 4.15 Distillation curve: (A) crude bio-oil 550 °C; (B) condensate; (C) distillate;

(D) stillage.
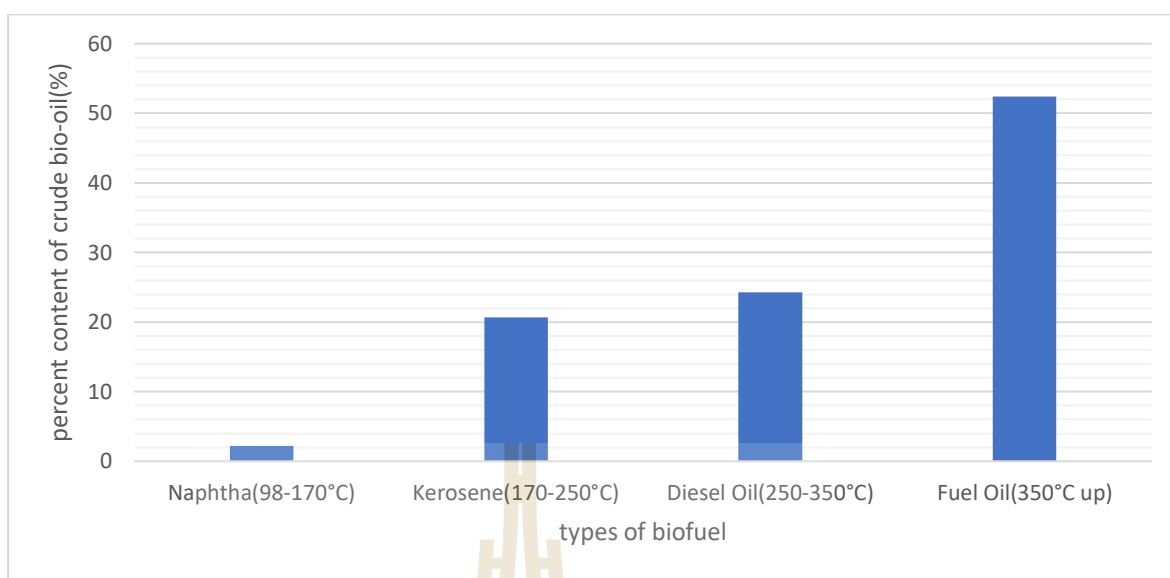
Figure 4.16 Percent content of crude bio-oil from optimal fast pyrolysis process at 550 °C.

Figure 4.17 Yield of products from short path distillation at 150 ºC, 10 mbar.
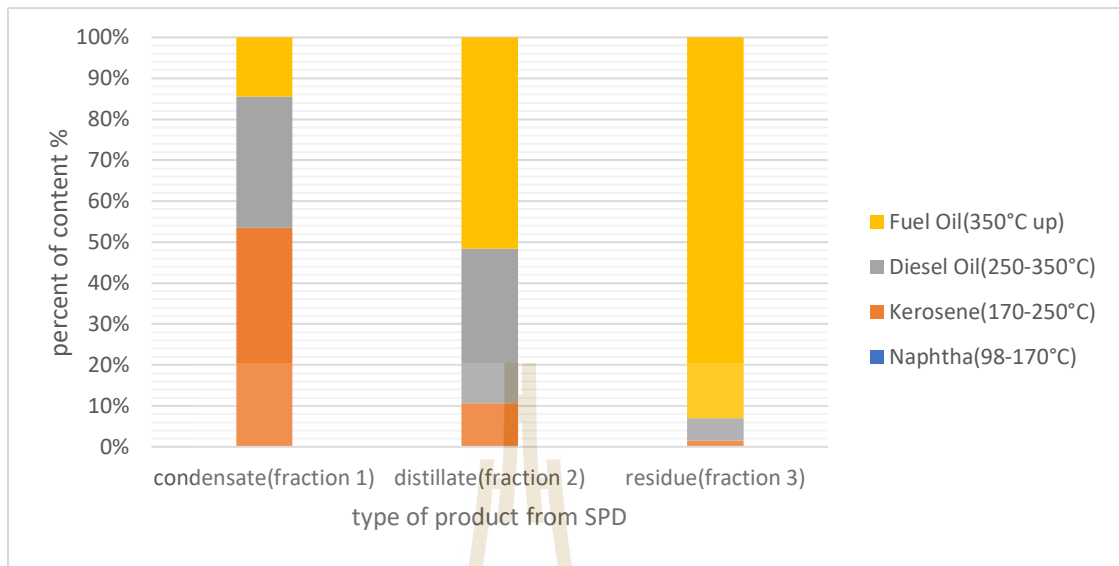
Figure 4.18 Percent content of each distillated product by short path distillation(SPD)

CHAPTER V

CONCLUSION

In this work, the process optimization of biofuel production from oleaginous yeast was studied. The *Rhodosporidium paludigena* yeast was culture in a 500-L by using cassava starch is substrate. Yeast was separated by using membrane separation. Then the spray drying was used for removal water from yeast. The bio-oil and biochar obtained from fast pyrolysis of yeast powder. The bio-oil was distillated at 150 °C by short path distillation.

Although yield of bio-oil was obtained of 60 % but this process was not suitable to produce kerosene or bio jet fuel because yield of kerosene was low. It was not worth for bio jet fuel production. Moreover, biochar yield at temperature 400 °C of 57.5 % could be enhanced by upgrading into activated carbon. This process has to be improved; for example, the high cell concentration could be fed in spray drying but cell concentration was low after membrane separation. The retentate should be concentrated by evaporation or sedimentation before feeding to spray drying unit. In fast pyrolysis unit, it should be continuous bed reactor even though feed of fluidize bed reactor might be blocked by packing of dried yeast powder.

REFERENCES

Al Arni, Saleh. 2018. 'Comparison of slow and fast pyrolysis for converting biomass into fuel', **Renewable Energy**, 124: 197-201.

Alam, Firoz, Saleh Mobin, and Harun Chowdhury. 2015. 'Third Generation Biofuel from Algae', **Procedia Engineering**, 105: 763-68.

Aljariri Alhesan, Jameel S., Yi Fei, Marc Marshall, W. Roy Jackson, Ying Qi, Alan L. Chaffee, and Peter J. Cassidy. 2018. 'Long time, low temperature pyrolysis of El-Lajjun oil shale', **Journal of Analytical and Applied Pyrolysis**, 130: 135-41.

Amaro, H. M., I. Sousa-Pinto, F. X. Malcata, and A. Catarina Guedes. 2017. '16 - Microalgal fatty acids—From harvesting until extraction.' in Cristina Gonzalez-Fernandez and Raúl Muñoz (eds.), **Microalgae-Based Biofuels and Bioproducts** (Woodhead Publishing).

Ambrosi, Alan, Nilo Cardozo, and Isabel Tessaro. 2014. 'Membrane Separation Processes for the Beer Industry: A Review and State of the Art', Food and **Bioprocess Technology**, 7.

Atadashi, I. M. 2015. 'Purification of crude biodiesel using dry washing and membrane technologies', **Alexandria Engineering Journal**, 54: 1265-72.

Beims, R. F., V. Botton, L. Ender, D. R. Scharf, E. L. Simionatto, H. F. Meier, and V. R. Wiggers. 2018. 'Effect of degree of triglyceride unsaturation on aromatics content in bio-oil', **Fuel**, 217: 175-84.

Ben Hassen Trabelsi, Aïda, Kaouther Zaafouri, Withek Baghdadi, Slim Naoui, and Aymen Ouerghi. 2018. 'Second generation biofuels production from waste cooking oil via pyrolysis process', **Renewable Energy**, 126: 888-96.

Bird, Michael, Claudia Keitel, and Will Meredith. 2017. 'Analysis of biochars for C,H,N,O and S by elemental analyser.' in.

Biswas, Bijoy, Rawel Singh, Bhavya B. Krishna, Jitendra Kumar, and Thallada Bhaskar. 2017. 'Pyrolysis of azolla, sargassum tenerrimum and water hyacinth for production of bio-oil', **Bioresource Technology**, 242: 139-45.

Bonturi, Nemailla, Leonidas Matsakas, Robert Nilsson, Paul Christakopoulos, Everson Miranda, Kris Berglund, and Ulrika Rova. 2015. 'Single Cell Oil Producing Yeasts Lipomyces starkeyi and Rhodosporidium toruloides: Selection of Extraction Strategies and Biodiesel Property Prediction', **Energies,** 8: 5040.

Breil, Cassandra, Alice Meullemiestre, Maryline Vian, and Farid Chemat. 2016. 'Bio-Based Solvents for Green Extraction of Lipids from Oleaginous Yeast Biomass for Sustainable Aviation Biofuel', **Molecules**, 21.

Bridgewater, Anthony. 2004. 'Biomass fast pyrolysis', **Thermal Science**, 8: 21-50.

Bridgwater, A. V., and G. V. C. Peacocke. 2000. 'Fast pyrolysis processes for biomass', **Renewable and Sustainable Energy Reviews**, 4: 1-73.

Chi, Chengdeng, Xiaoxi Li, Yiping Zhang, Song Miao, Ling Chen, Lin Li, and Yi Liang. 2020. 'Understanding the effect of freeze-drying on microstructures of starch hydrogels', **Food Hydrocolloids**, 101: 105509.

Chorn, L.G. 1984. 'Simulated Distillation of Petroleum Crude Oil by Gas Chromatography. Characterizing the Heptanes-Plus Fraction', **Journal of Chromatographic Science**, 22: 17-21.

Chowdhury, Zaira, Md Karim, Muhammad Ashraf, and Khalid Khalisanni. 2016. 'Influence of Carbonization Temperature on Physicochemical Properties of Biochar derived from Slow Pyrolysis of Durian Wood (Durio zibethinus) Sawdust', **Bioresources**, 11: 3356-72.

D. Mores, Wendy, and Robert H. Davis. 2002. Yeast-Fouling Effects in Cross-Flow Microfiltration with Periodic Reverse Filtration.

Eder, K. 1995. 'Gas chromatographic analysis of fatty acid methyl esters', Journal of Chromatography B: **Biomedical Sciences and Applications**, 671: 113-31.

Giri, S. K., and Suresh Prasad. 2007. 'Drying kinetics and rehydration characteristics of microwave-vacuum and convective hot-air dried mushrooms', **Journal of Food Engineering**, 78: 512-21.

Guedes, Raquel Escrivani, Aderval S. Luna, and Alexandre Rodrigues Torres. 2018. 'Operating parameters for bio-oil production in biomass pyrolysis: A review', **Journal of Analytical and Applied Pyrolysis**, 129: 134-49.

Gutiérrez-Antonio, C., F. I. Gómez-Castro, J. A. de Lira-Flores, and S. Hernández. 2017. 'A review on the production processes of renewable jet fuel', **Renewable and Sustainable Energy Reviews**, 79: 709-29.

Henao-Ardila, Alejandra, María Ximena Quintanilla-Carvajal, and Fabián Leonardo Moreno. 2019. 'Combination of freeze concentration and spray drying for the production of feijoa (Acca sellowiana b.) pulp powder', **Powder Technology**, 344: 190-98.

Her, Jiunn-Jye, and Ju-Sheng Huang. 1995. 'Influences of carbon source and C/N ratio on nitrate/nitrite denitrification and carbon breakthrough', **Bioresource Technology**, 54: 45-51.

Juang, Ruey-Shin, Huei-Li Chen, and Ying-Shr Chen. 2008. 'Membrane fouling and resistance analysis in dead-end ultrafiltration of Bacillus subtilis fermentation broths', **Separation and Purification Technology**, 63: 531-38.

Khoomrung, Sakda, Pramote Chumnanpuen, Suwanee Jansa-ard, Intawat Nookaew, and Jens Nielsen. 2012. 'Fast and accurate preparation fatty acid methyl esters by microwave-assisted derivatization in the yeast Saccharomyces cerevisiae', **Applied Microbiology and Biotechnology**, 94: 1637-46.

Kolouchová, Irena, Olga Maťátková, Karel Sigler, Jan Masák, and Tomáš Řezanka. 2016. 'Lipid accumulation by oleaginous and non-oleaginous yeast strains in nitrogen and phosphate limitation', **Folia Microbiologica**, 61: 431-38.

Kolouchová, Irena, Olga Maťátková, Karel Sigler, Jan Masák, and Tomáš Řezanka. 2016. 'Lipid accumulation by oleaginous and non-oleaginous yeast strains in nitrogen and phosphate limitation', **Folia Microbiologica**, 61: 431-38.

Kondoh, Hisaki, Kumiko Tanaka, Yuta Nakasaka, Teruoki Tago, and Takao Masuda. 2016. 'Catalytic cracking of heavy oil over TiO2–ZrO2 catalysts under superheated steam conditions', **Fuel**, 167: 288-94.

Kraisintu, P., W. Yongmanitchai, and Savitree Limtong. 2010. 'Selection and optimization for lipid production of a newly isolated oleaginous yeast, rhodosporidium toruloides DMKU3-TK16', **Kasetsart Journal - Natural Science**, 44: 436-45.

Krishnakumar, P., S. Suresh, and Baredar Prashant. 2016. 'A review on pyrolysis of protein rich microalgae biomass', **International Journal for Research in Applied Science and Engineering Technology**, 4: 327-31.

Lestander, Torbjörn A., Linda Sandström, Henrik Wiinikka, Olov G. W. Öhrman, and Mikael Thyrel. 2018. 'Characterization of fast pyrolysis bio-oil properties by near-infrared spectroscopic data', **Journal of Analytical and Applied Pyrolysis**, 133: 9-15.

Lestari, Lina, Viska Variani, I. Nyoman Sudiana, Dewi Sari, Wa Ilmawati, and Erzam Hasan. 2017. 'Characterization of Briquette from the Corncob Charcoal and Sago Stem Alloys', **Journal of Physics**: Conference Series, 846: 012012.

Li, Lixiong, Edward Coppola, Jeffrey Rine, Jonathan L. Miller, and Devin Walker. 2010. 'Catalytic Hydrothermal Conversion of Triglycerides to Non-ester Biofuels', **Energy & Fuels**, 24: 1305-15.

Li, Yonghong, Zongbao Zhao, and Fengwu Bai. 2007. 'High-density cultivation of oleaginous yeast Rhodosporidium toruloides Y4 in fed-batch culture', **Enzyme and Microbial Technology**, 41: 312-17.

Liu, Guangrui, Beibei Yan, and Guanyi Chen. 2013. 'Technical review on jet fuel production', **Renewable and Sustainable Energy Reviews**, 25: 59-70.

Liu, Jingxin, Simian Huang, Kai Chen, Teng Wang, Meng Mei, and Jinping Li. 2020. 'Preparation of biochar from food waste digestate: Pyrolysis behavior and product properties', **Bioresource Technology**, 302: 122841.

Maher, K. D., and D. C. Bressler. 2007. 'Pyrolysis of triglyceride materials for the production of renewable fuels and chemicals', **Bioresource Technology**, 98: 2351-68.

Maity, Sunil K. 2015. 'Opportunities, recent trends and challenges of integrated biorefinery: Part I', **Renewable and Sustainable Energy Reviews**, 43: 1427-45.

Mancio, A. A., S. A. P. da Mota, C. C. Ferreira, T. U. S. Carvalho, O. S. Neto, J. R. Zamian, M. E. Araújo, L. E. P. Borges, and N. T. Machado. 2018. 'Separation and characterization of biofuels in the jet fuel and diesel fuel ranges by fractional distillation of organic liquid products', **Fuel**, 215: 212-25.

Meng, Xin, Jianming Yang, Xin Xu, Lei Zhang, Qingjuan Nie, and Mo Xian. 2009. 'Biodiesel production from oleaginous microorganisms', **Renewable Energy**, 34: 1-5.

Monteiro, Ricardo Lemos, Bruno Augusto Mattar Carciofi, Antonio Marsaioli, and João Borges Laurindo. 2015. 'How to make a microwave vacuum dryer with turntable', **Journal of Food Engineering**, 166: 276-84.

Pan, Li-Xia, Deng-Feng Yang, Li Shao, Wei Li, Gui-Guang Chen, and Zhi-Qun Liang. 2009. 'Isolation of the Oleaginous Yeasts from the Soil and Studies of Their Lipid-Producing Capacities', **Food Technology and Biotechnology**, 47.

Pattiya, A. 2018. '1 - Fast pyrolysis.' in Lasse Rosendahl (ed.), Direct Thermochemical Liquefaction for Energy Applications (**Woodhead Publishing**).

Qiao, Kangjian, Syed Abidi, Hongjuan Liu, Haoran Zhang, Sagar Chakraborty, Nicki Watson, Parayil Ajikumar, and Gregory Stephanopoulos. 2015. 'Engineering lipid overproduction in the oleaginous yeast Yarrowia lipolytica', **Metabolic Engineering**, 29.

Qiao, Kangjian, Syed Hussain Imam Abidi, Hongjuan Liu, Haoran Zhang, Sagar Chakraborty, Nicki Watson, Parayil Kumaran Ajikumar, and Gregory Stephanopoulos. 2015. 'Engineering lipid overproduction in the oleaginous yeast Yarrowia lipolytica', **Metabolic Engineering**, 29: 56-65.

Santos, Andre L. F., Danilo U. Martins, Osvaldo K. Iha, Rafael A. M. Ribeiro, Rafael L. Quirino, and Paulo A. Z. Suarez. 2010. 'Agro-industrial residues as low-price feedstock for diesel-like fuel production by thermal cracking', **Bioresource Technology**, 101: 6157-62.

Shields-Menard, Sara A., Marta Amirsadeghi, W. Todd French, and Raj Boopathy. 2018. 'A review on microbial lipids as a potential biofuel', **Bioresource Technology**, 259: 451-60.

Sitepu, Irnayuli R., Luis A. Garay, Ryan Sestric, David Levin, David E. Block, J. Bruce German, and Kyria L. Boundy-Mills. 2014. 'Oleaginous yeasts for biodiesel: Current and future trends in biology and production', **Biotechnology Advances**, 32: 1336-60.

Sulaiman, F., and N. Abdullah. 2011. 'Optimum conditions for maximising pyrolysis liquids of oil palm empty fruit bunches', **Energy**, 36: 2352-59.

Taherian, Ali, Martin Mondor, and François Lamarche. 2015. "Enhancing quality of yellow peas." In.

Tai, Mitchell, and Gregory Stephanopoulos. 2013. 'Engineering the push and pull of lipid biosynthesis in oleaginous yeast Yarrowia lipolytica for biofuel production', **Metabolic Engineering**, 15: 1-9.

Thakur, M. S., S. G. Prapulla, and N. G. Karanth. 1989. 'Estimation of intracellular lipids by the measurement of absorbance of yeast cells stained with Sudan Black B', Enzyme and **Microbial Technology**, 11: 252-54.

Verma, Deepak, Bharat Singh Rana, Rohit Kumar, M. G. Sibi, and Anil Kumar Sinha. 2015. 'Diesel and aviation kerosene with desired aromatics from hydroprocessing of jatropha oil over hydrogenation catalysts supported on hierarchical mesoporous SAPO-11', **Applied Catalysis A: General**, 490: 108-16.

Wang, Jicong, Peiyan Bi, Yajing Zhang, He Xue, Peiwen Jiang, Xiaoping Wu, Junxu Liu, Tiejun Wang, and Quanxin Li. 2015. 'Preparation of jet fuel range hydrocarbons by catalytic transformation of bio-oil derived from fast pyrolysis of straw stalk', **Energy**, 86: 488-99.

Wang, Shurong, Yueling Gu, Qian Liu, Yan Yao, Zuogang Guo, Zhongyang Luo, and Kefa Cen. 2009. 'Separation of bio-oil by molecular distillation', **Fuel Processing Technology**, 90: 738-45.

Wang, Wei-Cheng, and Ling Tao. 2016. 'Bio-jet fuel conversion technologies', **Renewable and Sustainable Energy Reviews**, 53: 801-22.

Wang, Yunpu, Zihong Zeng, Xiaojie Tian, Leilei Dai, Ling Jiang, Shumei Zhang, Qiuhao Wu, Pingwei Wen, Guiming Fu, Yuhuan Liu, and Roger Ruan. 2018. 'Production of bio-oil from agricultural waste by using a continuous fast microwave pyrolysis system', **Bioresource Technology**, 269: 162-68.

Waqas, M., A. S. Aburiazaiza, R. Miandad, M. Rehan, M. A. Barakat, and A. S. Nizami. 2018. 'Development of biochar as fuel and catalyst in energy recovery technologies', **Journal of Cleaner Production**, 188: 477-88.

Xu, Lin, Jin-Hong Cheng, Peng Liu, Qian Wang, Zhi-Xiang Xu, Qing Liu, Jin-You Shen, and Lian-Jun Wang. 2019. 'Production of bio-fuel oil from pyrolysis of plant acidified oil', **Renewable Energy**, 130: 910-19.

Yimyoo, Teera, Wichien Yongmanitchai, and Savitree Limtong. 2011. Carotenoid Production by Rhodosporidium paludigenum DMKU3-LPK4 using Glycerol as the Carbon Source.

Zhang, Shuyan, Masakazu Ito, Jeffrey M. Skerker, Adam P. Arkin, and Christopher V. Rao. 2016. 'Metabolic engineering of the oleaginous yeast Rhodosporidium toruloides IFO0880 for lipid overproduction during high-density fermentation', **Applied Microbiology and Biotechnology**, 100: 9393-405.

Zhang, Yajing, Peiyan Bi, Jicong Wang, Peiwen Jiang, Xiaoping Wu, He Xue, Junxu Liu, Xiaoguo Zhou, and Quanxin Li. 2015. 'Production of jet and diesel biofuels from renewable lignocellulosic biomass', **Applied Energy**, 150: 128-37.

Zhenyi, Cheng, J. I. Xing, L. I. Shuyuan, and L. I. Li. 2004. 'Thermodynamics Calculation of the Pyrolysis of Vegetable Oils', **Energy Sources**, 26: 849-56.

BIOGRAPHY

Mister Pongsatorn Poopisut was born on June 1, 1992 in Nakhon Ratchasima, Thailand. He graduated with a Bachelor of Chemical engineering from Suranaree University of Technology in 2016. Then, He worked with Assoc. Prof. Dr.Apichat Boontawan before he studied Master of Science in school of Biotechnology, Institute of Agricultural Technology, Suranaree University of Technology (SUT) with Assoc. Prof. Dr.Apichat Boontawan. He received a Graduate scholarship from SUT to support him tuition and fee. In 2017, His research consisted of process optimization of fast pyrolysis of yeast oil for the biofuel production.

Presentation

Pongsatorn Poopisut, Chotika Gosalawit , Mariena Ketudat-Cairns, Apichat Boontawan 2019 (Oral oresentation) Fermentation of an Oleaginous Yeast *Rhodosporidium paludigenum* for biofuels production. 2019 International conference on on green energy systems (ICGES 2019); 2019 oct 9-11; Bangkok, Thailand.

Manuscript in preparation

Pongsatorn Poopisut, Chotika Gosalawit , Mariena Ketudat-Cairns, Apichat Boontawan 2019. Fermentation of an Oleaginous Yeast *Rhodosporidium paludigenum* for biofuels production. International Journal of Smart Grid and Clean , v9, n 6, November 2020.